ABSENCE OF INTERLEUKIN-6 PROTECTS BONE MARROW ERYTHROID RECOVERY UNDER INFLAMMATION, A PROCESS INHIBITED BY IRON MEDIATED ROS (REACTIVE OXYGEN SPECIES) UPREGULATION

A Dissertation
Presented to the Faculty of the Weill Cornell Graduate School
of Medical Sciences
in Partial Fulfillment of the Requirements for the Degree of
Doctor of Philosophy

By
Ritama Gupta
June 2017

ABSENCE OF INTERLEUKIN-6 PROTECTS BONE MARROW ERYTHROID RECOVERY UNDER INFLAMMATION, A PROCESS INHIBITED BY IRON MEDIATED ROS (REACTIVE OXYGEN SPECIES) UPREGULATION
Ritama Gupta, Ph.D.
Cornell University 2017

Inflammatory states seen in infection and chronic disorders are often characterized by a condition called anemia of inflammation (AI). The iron deficiency in AI is predominantly due to an altered balance of the cytokine, Interleukin-6 (IL6) and the hormone hepcidin (Hamp). We have previously shown that lack of IL6 or Hamp in knockout mouse models (*IL6*-KO, *Hamp*-KO) injected with the heat-killed pathogen *Brucella abortus* (BA) results in improved recovery from anemia. However, BM erythroid recovery in *IL6*-KO mice was far more improved in comparison to the iron overloaded *Hamp*-KO mice. This prompted us to investigate cellular responses driving BM erythropoiesis under inflammation in *IL6*-KO mice and the effect of iron overloading conditions on erythroid recovery under condition of AI. To address these questions, we generated a double knock out for *IL6* and *Hamp* (DKO) and investigated BM erythropoiesis in WT, *IL6*-KO, *Hamp*-KO and DKO mice.

The erythroid recovery in the BM of these mice were characterized by two phases. During the first phase (in the first 72 hours following BA administration), all the mice showed impaired BM erythropoiesis. Analysis of WT and *IL6*-KO mice indicated that impaired BM was associated by a surge in inflammatory cytokines such as IFNγ and TNFα and a concurrent increase in mitochondrial ROS. Following 72 hours BM erythropoiesis recovered in the BM: compared to WT and *Hamp*-KO, BM erythropoiesis was qualitatively and quantitatively better in *IL6*-KO animals, showing the best profile in DKO mice. During the second phase (10 to 14-day post BA administration), we observed a second surge of inflammatory cytokines. During this phase, we observed a severe regression of BM erythropoiesis in DKO mice, while *IL6*-KO animals continued to show an excellent profile.

During the second phase, we also observed that, while WT mice upregulated mitochondrial ROS, *IL6*-KO animals did not. We showed that ROS upregulation is triggered by erythropoietic stress (as seen in WT animals recovering after phlebotomy). However, we also postulated that inflammation and iron overload can further increase oxidative stress in erythroid cells, and that excessive ROS upregulation impairs erythroid recovery. Hence, BM erythropoiesis in *IL6*-KO mice is improved by reduced ROS formation in presence of inflammatory cytokines. However, if our model is correct, administration of iron to *IL6*-KO animals should impair BM erythropoiesis during the second phase as seen in DKO. In fact, iron administration impaired BM erythropoiesis in *IL6*-KO mice and, concurrently, increased ROS in erythroid cells. In accordance with our model, during the second phase also DKO and *Hamp*-KO mice showed increased ROS in BM erythroid cells. We are currently investigating which form of iron is responsible for this mechanism (labile iron pool versus transferrin bound iron) and what the role of IL6 is in this process.

BIOGRAPHICAL SKETCH

Ritama received her Bachelor of Science in Microbiology from St. Xavier's college, University of Calcutta, at Kolkata, India. She joined the PhD program in Immunology and Microbial Pathogenesis at Weill Cornell Graduate School of Medical Sciences in the fall of 2011 and subsequently started work in the Rivella lab on erythropoietic disorders. She currently works as an *in abstentia* graduate student with Dr. Stefano Rivella at the University of Pennsylvania and The Children's Hospital of Philadelphia; investigating the role of Interleukin 6 and Hepcidin in a mouse model of anemia of inflammation.

DEDICATION

This doctoral dissertation is dedicated to my late grandmother Smt. Gauri Gupta. This PhD would not have been possible without her constant support of my educational goals and I know she would be proud of me today.

I would like to thank my parents Raja Gupta and Rajashi Gupta, who have worked tirelessly and made innumerable sacrifices throughout their lives to help me get to where I am today. Thank you for teaching me the strength of humility, hard work, discipline, and perseverance.

I would like to share this PhD with my brother Dot- my friend, my helping hand, my confidant for life. Thank you for having faith in me, when I didn't have faith in myself.

I am also grateful for my childhood best friend Maddy-our friendship has survived the test of time and distance, and I know I would not have been able to begin and complete this chapter of my life without your support.

My utmost gratitude to my PhD mentor Dr. Stefano Rivella. Your kindness on one hand and positive criticism on the other, have made this PhD possible. It has been an honor to learn and work under your guidance.

Thank you to my graduate school best friends-Alisa and Dane. Right from the beginning, we have carried each other, through hurdles both professional and personal. Some of my most cherished moments in graduate school have you two in it, and I will carry them with me for the rest of my life.

Roberta, your scientific assistance has been instrumental in bringing my PhD thesis to completion, thank you for that, and also for your friendship that has shaped my life in lab. Truly, my time in lab has been infinitely brighter in your presence. Thank you to Carla, for teaching me everything about mouse work, I owe my skill and knowledge of handling animals to your guidance. I am also indebted to Sara, for introducing this project to me, and for her elegant work on the Brucella model that has been the foundation of my project. Every past and previous member of my lab that I have had the pleasure of working with has contributed to this PhD, and I am very grateful for it.

I would also like to extend my gratitude to my first teacher in Immunology, Kasturi Ma'am and the head of the department of Microbiology at my alma mater St. Xavier's College, Kolkata-AKM sir. Your lessons inspired me to pursue scientific

research. Some of the most inspiring figures in my life in India have been teachers. But none have inspired me as much as you have, Riddhi sir. Thank you for your kindness, and support. I felt the first shadow of having a professional mentor in you and in our conversations at St. Xavier's.

Last but not the least, I would like to thank my fur friend and baby Lavender. You came into my life at a time when I needed a friend the most and you have captured my heart with your undying love. I know that this milestone in my life has been made ever so special by your presence.

Thank you to every person, stranger, family or friend; whose random acts of kindness have helped me push through the past six years and bring this chapter of my life to completion.

ACKNOWLEDGEMENT

TABLE OF CONTENTS

LIST OF FIGURES

LIST OF ABBREVIATIONS

AI	Anemia of Inflammation
AP-2	Adaptor Protein -2
ADP	Adenosine Di Phosphate
atg8	autophagy related protein 8
ATP	Adenosine Tri Phosphate
BA	*Brucella abortus*
BFU-E	Burst Forming Unit- Erythroid
BM	Bone Marrow
BMP	Bone Morphogenic Protein
CEBP-α	CCAAT Enhancer binding protein α
CFU-E	Colony Forming Unit-Erythroid
CFA	Complete Freud's Adjuvant
CHOP	CEBP Homologous protein
CLP	Cecal Ligation and Puncture
DAMP	Damage associated Molecular Pattern
Dcytb	Duodenal cytochrome b
DMT1	Divalent Metal ion Transporter
DNA	Deoxyribonucleic Acid
ER	Endoplasmic Reticulum
ETC	Electron Transport Chain
G-csf	Granulocyte-colony stimulating factor
gp80	glycophorin 80
***Hamp*-KO**	Hepcidin-knock out
HFE	High Fe hemochromatosis protein
HIF	Hypoxia inducible factor
HIV	Human Immunodeficiency Virus
HSC	Hematopoietic Stem Cell
IFNγ	Interferon γ
IL6	Interleukin 6
***IL6*-KO**	Interleukin 6- knock out
IP	Intraperitoneal
IRE	Iron Restricted Erythropoiesis
JAK	Janus Kinase
KEAP1	Kelch like ECH Associated Protein-1
LC3	Microtubule associated Light Chain 3
MAPK	Mitogen Associated Protein Kinase
M-csf	Monocyte-colony stimulating factor

MLKL	Mixed Lineage Kinase Domain Like Pseudokinase
mPTP	Mitochondrial Permeability transition pore
mRNA	Messenger Ribonucleic Acid
NADH	Nicotinamide Adenine Dinucleotide reduced
NFκB	Nuclear Factor κB
NLR	Nod Like Receptor
NLRP3	NLR family Pyrin domain containing 3
Nramp-1	Natural resistance associated macrophage protein-1
NRF2	Nuclear factor erythroid 2 related Factor 2
NTBI	Non-Transferrin Bound Iron
PAMP	Pathogen Associated molecular pattern
RBC	Red Blood Cell
RIPK1	Receptor Interacting Serine/Threonine kinase 1
RNA	Ribonucleic Acid
ROS	Reactive Oxygen Species
SOD1	Superoxide Dismutase 1
STAT3	Signal Transducer and Activator of Transcription 3
Tf	Transferrin
TfR1	Transferrin Receptor 1
TGFβ	Transforming growth factor β
TLR	Toll like receptor
TMPRSS6	Transmembrane Protease Serine 6
TNFα	Tumor necrosis factor α
TNFR	Tumor necrosis factor α Receptor
TRAF2	TNF Receptor Associated Factor 2
WT	Wild Type
ZIP8	Zrt and Irt like Protein 8

Chapter One

Introduction

Erythrocytes are the primary carrier of oxygen in vertebrate systems. They are generated from multipotent HSCs mostly in the bone marrow of adult vertebrates by a process known as Hematopoiesis. Oxygen carrying capacity of erythrocytes stems from their key constituent Heme, capable of binding to iron and delivering oxygen to tissue through circulating RBCs. As a result, erythropoiesis and iron levels are tightly linked in mammalian systems in order to maintain a healthy balance of iron utilization for generation of new erythroblasts and iron recycling from senescent erythrocytes.

Iron has some unique properties that makes it crucial to the functioning of the mammalian physiological system. One such property is its interconversion from ferric (Fe^{3+}) to ferrous (Fe^{2+}) form [1]. While this makes iron an essential component of oxygen carrying proteins like Hemoglobin and Myoglobin, as well as many redox enzymes, it also allows iron to generate harmful oxidative radicals [2]. This dichotomous nature of Iron functioning requires this element to be tightly regulated. A careful balance of iron absorption and iron discharge is maintained in mammals, to simultaneously utilize iron for

physiological benefits and circumvent its potentially harmful properties. Loss of this balance is the underlying cause of many disorders, with symptoms ranging from anemia to hemochromatosis (iron overload). Although many of these disorders have been identified and some characterized, their underlying molecular mechanisms have only recently begun to be elucidated.

AI, also known as anemia of chronic diseases, is believed to be the second most common cause of anemia after iron deficiency anemia (3). It affects patients with both acute and chronic inflammation, seen in infections, malignancies and autoimmune disorders (4, 5, 6). A substantial proportion of patients suffering from acute or chronic infections are affected by AI. These infections include HIV, hepatitis C virus, diseases like tuberculosis, and others (7, 8, 9). Along with infections, cancer patients also exhibit symptoms of AI. Within autoimmune disorders, AI can affect patients with rheumatoid arthritis, inflammatory bowel disorder and systemic lupus erythematous (5, 10, 11). AI has also been reported in cases of chronic kidney disease, cardiovascular disease and in patients with rejection following an organ transplant (12, 13, 14). While in the case of acute AI, prognosis is directly linked to clearance of the pathogen from the body, in chronic AI, symptoms worsen with disease progression, thereby affecting treatment and management options. Therapies geared towards treating the anemia with iron supplements are not only ineffective in some cases, but can also be detrimental when iron allows the pathogen to thrive, as is the case in many infections (15). Thus, understanding the cellular mechanisms of

dysregulated iron metabolism, which contribute to AI, is critical for designing

effective cures

Erythroid differentiation and generation of RBCs

Erythropoiesis

Erythropoiesis is the process in which HSCs proliferate and differentiate to

generate enucleate erythrocytes or RBCs. It occurs in two phases: proliferation of

erythroid progenitors and terminal erythroid differentiation. In the first phase of

erythroid progenitor proliferation, multipotent HSCs will proliferate and

differentiation into BFU-E which in turn gives rise to CFU-E (16). Terminal

erythroid differentiation starts at the pro-erythroblast stage. This stage undergoes

three consecutive mitosis to generate basophilic erythroblast followed by

polychromatic erythroblast and then orthochromatic erythroblasts. Generally, one

pro-erythroblast gives rise to 2 basophilic erythroblasts, these 2 basophilic

erythroblasts will create 4 polychromatic erythroblasts and then the latter

undergoes further mitosis to give 8 orthochromatic erythroblasts thereby

maintaining a 1: 2: 4: 8 ratio from the pro-erythroblast to the orthochromatic

erythroblast stage (17). The othorchromatics expel their nuclei to generate

reticulocytes which undergo further changes to give rise to erythrocytes or RBCs.

Terminal erythroid differentiation is accompanied by a decrease in expression of

certain cell surface proteins, decrease in cell size, changes in organization of membrane structure, chromatin condensation and hemoglobinization during the transition from the pro-erythroblast to the RBC stage (17).

Characterization of progenitor populations in terminal erythroid differentiation

The two major sites of erythropoiesis in adult mammals are the BM and the spleen. Terminal erythroid differentiation in the murine BM and spleen has been extensively characterized by distinguishing individual progenitor populations by expression of cell surface makers using flow cytometry, morphological features by cytospins and genetic characteristics by RNA sequencing (17, 18). The most widely accepted and adaptable method of identifying erythroid progenitor populations is by using the cell surface erythroid marker TER119. Cells expressing TER119 can be distinguished into each progenitor population by difference in expression of CD44. Beginning from the pro erythroblast stage each subsequent population undergoes a decrease in expression of CD44 and shrinks in size to give rise to RBCs (Figure 1). Another marker used in identifying progenitor populations is CD71. Early in terminal erythroid differentiation erythroid progenitors are TER119$^+$CD71$^+$ while RBCs are TER119$^+$CD71$^-$ (Figure 1).
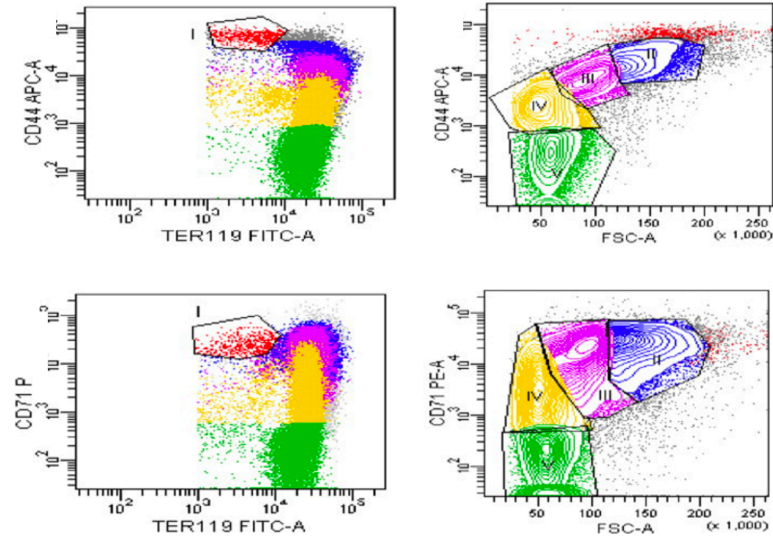
Figure 1.1. Terminal erythroid differentiation resolved by expression of TER119, CD71 and CD44. (I) Pro-erythroblast, (II) Basophilic erythroblast (III) Polychromatic erythroblasts (IV) Orthochromatic erythrobalst and reticulocyte (V) RBCs. Adapted and modified from Chen *et al*.

Iron metabolism and its regulation

Iron homeostasis

The majority of iron in the mammalian body is located in hemoglobin, which is the predominant protein in erythrocytes (or RBCs). Plasma also contains iron, where it is maintained in the soluble form by binding to the glycoprotein Tf, which supplies it to cells like developing erythrocytes, hepatocytes and placental trophoblasts by binding to the transmembrane Tf receptor on the cell surface (19, 20, 21, 22). The level of Tf saturation can in certain cases be used as an indicator of iron deficiency or iron overload. Very low Tf saturation implies iron deficiency, while excessive saturation of Tf signals iron overload. When the

5

amount of iron present exceeds the amount of Tf available for binding, which occurs in cases of exceedingly high Tf saturation (23). It gives rise to NTBI, which can cause oxidative damage to cells (24, 25). A component of this NTBI forms the labile plasma iron which constitutes the labile iron pool within the plasma (26). Although the labile iron pool consists of chelatable redox active iron, when tightly regulated and maintained at low levels this serves a homeostatic role in iron metabolism. However, in conditions of iron overload, dysregulated expansion of the labile iron pool causes labile plasma iron to enter into cells and tissues, causing damage through oxidative stress (27, 28). There are certain metal ion transporters such as ZIP8 implicated in iron transport (29). This transporter could potentially be capable of taking up this excess iron within a labile iron pool, not bound to transferrin-for supply to erythroid progenitors, subsequently extending the arm of NTBI mediated oxidative damage to erythroid differentiation. Whether conditions of NTBI are accompanied by dysregulated expression of ZIP transporters remains to be seen.

Majority of this Tf bound plasma iron comes from daily recycling of senescent erythrocytes with the hemoglobin/haptoglobin scavenger receptor (CD163) (30). A small fraction of this is also derived from dietary iron. In duodenal enterocytes lining the absorptive villi, dietary iron is taken up in the ferric form with the help of a transporter called DMT1 and the enzyme ferric reductase, or Dcytb which reduces it to the ferrous form for cellular uptake (31, 32). Plasma iron levels are also maintained through iron recycling by macrophages that phagocytose dying or senescent erythrocytes, extract iron

from the hemoglobin by catabolizing Heme via the hemoxygenase enzyme, and release it into circulation (33, 34). Release of stored iron from hepatocytes and placental transport of iron from the mother to the fetus also contribute to Tf bound plasma iron levels. Although there are multiple ways to import iron, cellular iron export occurs through the only known iron exporter-ferroportin wherein enzymes like ceruloplasmin or hephaestin oxidize the ferrous iron to ferric form following Ferroportin mediated export and preceding plasma Tf loading (35, 36, 37, 38) (Figure 2).
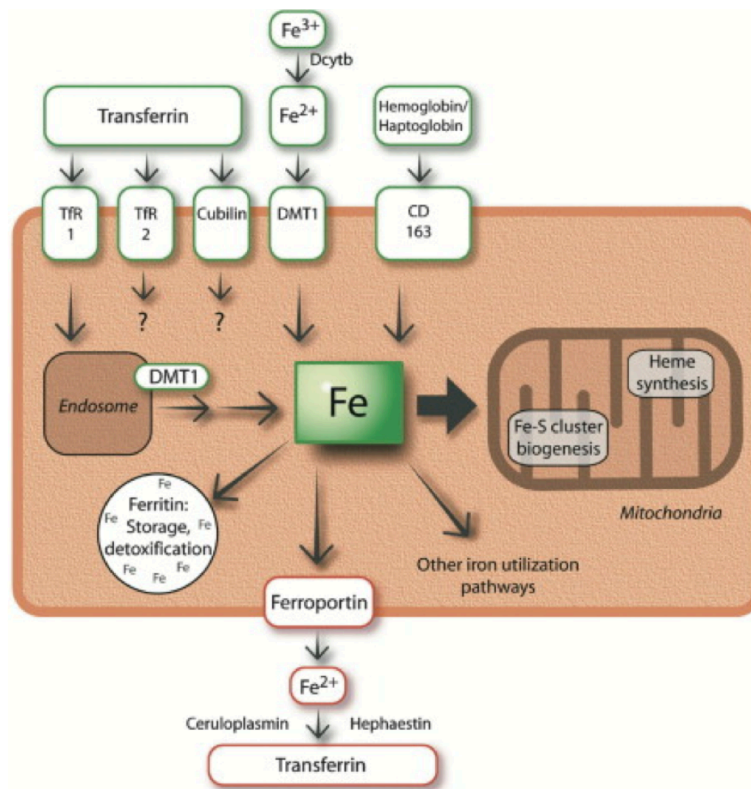
Figure 1.2. Cellular iron homeostasis. Adapted from Hentze *et al*.

Ferroportin is highly expressed on the cell membrane of hepatocytes, macrophages, duodenal enterocytes and placental trophoblasts.

Hepcidin

Hepcidin is considered a key regulatory molecule of systemic iron homeostasis. This 25 amino acid peptide hormone is produced primarily by hepatocytes (39, 40). Hepcidin acts as a negative regulator of iron availability by preventing export of iron absorbed by duodenal enterocytes, stored iron from hepatocytes, recycled iron from phagocytizing macrophages and transported iron on placental trophoblasts. This produces immediate hypoferremia as evidenced by studies where a single dose of 50 ug of Hepcidin in mice caused a rapid drop in serum iron in 1 hour (41). Hepcidin carries out this negative regulation of iron availability by directly binding to the iron exporter ferroportin. This binding elicits internalization of the hepcidin-ferroportin complex and its consequent ubiquitylation and degradation in lysosomes (42, 43, 44). In a feedback loop, Hepcidin in itself is also regulated by the element it controls: iron. This happens such that when iron levels are plentiful, Hepcidin expression is upregulated. Circulating hepcidin binds and degrades ferroportin on the basolateral side of duodenal enterocytes thereby preventing release of absorbed iron into plasma. It also concurrently degrades Ferroportin on Macrophages and hepatocytes further lowering plasma iron supply (Figure 3). Conversely, under conditions of iron deficiency, Hepcidin expression is downregulated, releasing iron into circulation thereby increasing Tf saturation and plasma iron levels (45, 46, 47, 48).
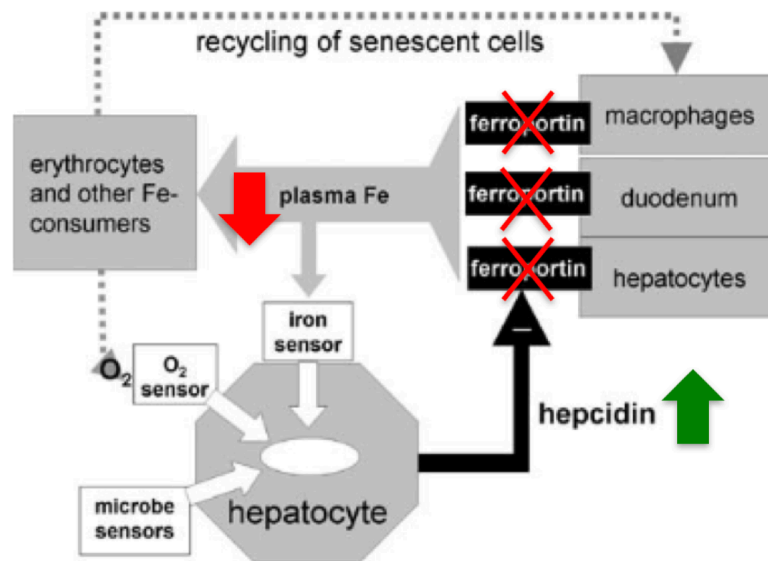
Figure 1.3. Role of Hepcidin in negative regulation of iron availability. Adapted and modified from Nemeth *et al*.

There are multiple factors that regulate expression of Hepcidin in the mammalian physiological system. One such factor is iron availability. This is mediated by the membrane protein HFE. Under conditions of high serum iron and Tf-saturation, the membrane protein HFE, generally sequestered away by binding to TfR1 (Transferrin receptor 1) is displaced to TfR2 (Transferrin receptor 2) thereby forming an Fe-Tf, HFE, TfR2 complex. This complex has been implicated in upregulating transcription of Hepcidin (49, 50, 51). It can do so independently or in concert with the BMP-SMAD pathway, the key pathway in inducing expression of Hepcidin. BMP6, belonging to the TGFβ superfamily of proteins binds to the BMP receptor I and II complex including the BMP coreceptor Hemojuvelin which confers sensitivity of binding. Activation of the BMP receptor leads to phosphorylation of SMAD1/5/8 in the cytosol and the latter

then goes on to interact and form a complex with SMAD 4 which translocates to the nucleus and induces expression of Hepcidin (52, 53, 54, 55). A serine protease Matriptase -2 encoded by the TMPRSS6 gene is capable of cleaving the BMP coreceptor Hemojuvelin, negatively regulating expression of Hepcidin such that TMPRSS6$^{-/-}$ mice have severe iron deficiency anemia (56, 57, 58). On the other side of the spectrum, mutations in gene contributing to Hepcidin expression, such as HFE, TfR2 and those within Hepcidin itself, can lead to conditions of iron overload, and are the central causes of hereditary hemochromatosis in clinical settings (47, 49).

Another factor controlling Hepcidin expression is Hypoxia and erythropoietic activity (59). It has been shown in vitro that HIF1 and HIF2 downregulates Hepcidin expression via upregulation of erythropoietin (60,). In vivo, it has been shown that stimulating erythropoiesis either by treatment with Erythropoietin or by phlebotomy to cause rapid anemia triggers an expansion of erythroid progenitors and a concurrent downregulation of Hepcidin expression (61). Since erythroid progenitors are the primary consumers of plasma iron, to prevent depletion of plasma iron levels under conditions when expansion of the erythroid progenitor pool is necessary, e.g. stress or ineffective erythropoiesis, erythropoietin treatment etc., these erythroid progenitors produce an erythroid factor named "Erythroferrone" which suppresses hepcidin expression. How erythroferrone acts on hepatocytes to suppress hepcidin remains to be elucidated. Upregulation of this factor is the primary cause of iron overload seen in genetic disorders of secondary hemochromatosis manifesting ineffective

erythropoiesis, such as β thalassemia (61, 62, 63).

The final factor that controls Hepcidin expression is inflammation. In acute, as well as in chronic inflammatory conditions, infections, autoimmune disorders, or malignancies, hypoferremia associated with upregulated Hepcidin expression has been observed. The most important cause of this is the production and upregulation of cytokines such as IL1 and IL6, which have been implicated in the increase of Hepcidin levels. Aside from pro inflammatory cytokines, ER stress has also been linked to upregulated Hepcidin levels (64, 65).

Inflammation

The general inflammatory reaction

Inflammation is considered to be an adaptive biological reaction to a disruption in tissue homeostasis (66). The primary aim of inflammation is in resolution of damage, and hence beneficial, for example, in the context of an infection. However, dysregulated inflammation can be injurious, for example, in autoimmune disorders. The general inflammatory pathway follows a sequence of inducers, sensors, mediators and effectors (66). Primary exogenous microbial inducers of inflammation include PAMPs expressed by a multitude of receptors on cells participating in the inflammatory response. Endogenous inducers include DAMPs released by previously infected cells that can further progress the

inflammatory reaction (67, 68). The first responding cells at the site of entry of a pathogen or damage to tissue, are part of the innate response. These include macrophages, neutrophils and mast cells that express PAMP and DAMP recognizing receptors such as NLRs and TLRs, which are the sensors (69, 70, 71, 72). Activation of these receptors, the latter in particular, can trigger the rapid activation of the transcription factor NFκB which then translocates to the nucleus and induces expression of target genes (73, 74). This includes a variety of chemokines, cytokines, eicosanoids, vasoactive amines etc., also known as the mediators (66). These form the very first phase of response at the site of damage. Additionally, chemokines generated also allow further extravasation of leukocytes to the site of infection (75, 76). Depending on the degree and intensity of damage, the inflammation maybe be resolved by this initial response, or may be continued by further infiltration of macrophages, and adaptive immune cells. When the initial responders are capable of limiting the damage, a resolution phase ensues through clearance of debris and dead cells, transition from the pro-inflammatory state to an anti-inflammatory state and replacing the area of damage by tissue remodeling (77).

IL6

IL6, though initially considered as a pro-inflammatory cytokine, has been shown to have pleiotropic functions regulating a multitude of cellular processes (78). On binding to the IL6 receptor (gp80) associated with the signal transducer (gp 130) it can induce the phosphorylation and activation of the transcription

factor STAT3 which translocates to the nucleus and stimulate expression of target genes (79, 80). IL6 is produced by all cells of the mononuclear phagocytic system, as well as by adaptive immune cells. Aside from its role in the initial response to invading pathogens and tissue damage during acute inflammatory reactions, this cytokine has been implicated in differentiation of multiple T helper cell subsets, in acute phase response by inducing expression of acute phase proteins, in osteoblast maturation, in hematopoiesis within the bone marrow and in inducing anemia under inflammation, among others (81, 82, 83, 84).

TNFα

TNFα is a key inflammatory mediator present both as a soluble and membrane bound form and capable of binding to TNF receptor 1 and 2. On binding, the latter is cleaved by membrane metalloproteinases into an activated form. The activated receptors can trigger downstream signaling pathways through TRAF2 to induce activation of AP-2 and NFκB among other factors that are able to upregulate the expression of multiple inflammatory mediators including TNFα itself (85, 86). This cytokine is primarily expressed by macrophages, but can also be secreted by other cells of both innate and adaptive immune responses. Apart from its role as an inflammatory mediator, an important function of TNFα is inducing expression of chemokines that allow extravasation of mononuclear phagoyctes, from blood vessels to the site of tissue damage or infection as first responders to an inflammatory reaction (87). In

addition to this, TNFα has also been linked to caspase-8 mediated apoptosis, non-apoptotic programmed cell death such as necroptosis, lipid metabolism, differentiation of T helper cell subsets and in maintenance of endothelial cell function (88, 89, 90, 91).

IFNγ

Expression of many inflammatory mediators, including the two mentioned above, is regulated by IFNγ. This cytokine is capable of priming macrophages either synergistically with activated TLRs to stimulate NFκB activation or independently through the phosphorylation and activation of STAT1(92). IFNγ primed macrophages upregulate expression of over 200 genes including G-Csf, M-Csf and IL12-p40. INFγ has also been implicated in inhibiting the expression of IL10, and can, in certain cases, contribute to exaggerated chronic inflammatory conditions such as inflammatory bowel disease and lupus (93, 94, 95).

Mitochondria, oxidative stress and cell death

Mitochondria

Health and survival of a mammalian cellular system requires the coordinated functioning of its intracellular organelles to recognize external cues and respond appropriately. Mitochondria are double membrane bound endosymbiotic organelles capable of acting as the ultimate "responsive sensing

14

system" by detecting alterations and functioning accordingly (96). Although the classical function of energy homeostasis has caused these organelles to be aptly named as the "powerhouse of the cell", mitochondria have also been implicated in a host of other functions, including but not limited to inter-organelle signaling, responding to cytokine cues, calcium homeostasis, activation of the inflammasome, generation of ROS and cell death (96).

Mitochondria consists of two functionally distinct outer and inner membranes separated by an inter membrane space and encapsulating the mitochondrial matrix, housing among various other factors, a circular mitochondrial DNA encoding certain components of the ETC (97). Sensing of metabolites such as glucose and fatty acids results in subsequent oxidative phosphorylation which converges on the ETC to generate an electrochemical gradient across the inner mitochondrial membrane, energy in the form of ATP, water and ROS. Multiple megacomplexes of iron-sulfur clusters comprise the ETC which consists of complex I (NADH dehydrogenase), ubiquinone, complex II (succinate dehydrogenase), complex III (bc_1 complex), cytochrome c, complex IV (cytochrome c oxidase) and ATP synthase. Electron transfer along the ETC is initiated when pyruvate generated from Glucose by Glycolysis is converted to Acetyl CoA in the Mitochondria by Pyruvate Dehydrogenase. Acetyl CoA is also produced from β-oxidation of Fatty Acids. Metabolite derived Acetyl CoA enters into the Krebs Cycle to produce electron donors like NADH accepted by complex I of the ETC to initiate transfer of electrons (98, 99, 100, 101). As electrons flow down the ETC, this gradient of electrons pumps protons or hydrogen ions from

the mitochondrial matrix across the inner mitochondrial membrane, giving rise to

an electrochemical gradient across the membrane called mitochondrial

membrane potential ($\Delta\psi$m) (102). Subsequently these protons re-enter the

mitochondrial matrix through the ATP synthase to form water while the ATP

synthase itself utilizes the proton gradient to give rise to ATP from ADP and

inorganic phosphate such that 36 ATP molecules are produced per molecule of

glucose that is metabolized. Although majority of the electrons flow down the

ETC and are involved in the generation of ATP, a few electrons are leaked and

can react with oxygen at certain complexes of the ETC itself to generate

oxidative radicals or ROS (103, 104).

ROS and oxidative stress

A small fraction of electrons moving down the ETC can generate ROS by

the one electron reduction of oxygen at complexes of the ETC. ROS refers to

non-radical oxidants such as hydrogen peroxide (H_2O_2) and singlet oxygen ($^1O_2$)

as well as free radicals such as superoxide anion ($O_2^{.-}$) and hydroxyl radical

($^.OH$) (105, 106, 107, 108). Incomplete reduction of molecular oxygen at

complexes I and III gives rise to the most abundant form of ROS called

superoxide anion ($O_2^{.-}$) on the mitochondrial matrix side of the inner

mitochondrial membrane (Figure 4). The steady state concentration of the

superoxide anion ($O_2^{.-}$) is about 5-10 fold higher within the mitochondrial matrix

than it is in the cytosol or other organelles (109, 110, 111). These levels of

superoxide anion ($O_2^{.-}$) which can otherwise damage iron sulfur clusters within

16

complexes of the ETC, are tightly regulated by the presence of enzymes such as SOD1 residing in the mitochondrial intermembrane space and SOD2 residing in the mitochondrial matrix (112). For this reason, high levels of superoxide anion ($O_2^{\cdot-}$) are generally related to a decline in mitochondrial health than with steady state redox signaling. Mitochondrial respiration is the primary source of ROS because the Superoxide anion ($O_2^{\cdot-}$) is capable of generating most other forms of ROS. Spontaneous or enzymatic dismutation of superoxide anion ($O_2^{\cdot-}$) gives rise to hydrogen peroxide (H_2O_2) (Figure 4). The latter in turn can react with Superoxide anion ($O_2^{\cdot-}$) through ferrous ion catalyzed Fenton reaction as well as the Haber Weiss reaction to generate the most aggressive oxidant, the hydroxyl radical ($^{\cdot}OH$) (113, 114, 115, 116). This potent form of ROS is capable of indiscriminately oxidizing proteins, lipids and DNA contributing to genomic instability and ultimately cell death. For this reason, there are elegant scavenging systems in place to maintain ROS at low levels (117). While all of these forms of ROS have varying degrees of reactivity, under physiological conditions ROS production constitutes a very small proportion of mitochondrial oxygen consumption, and as mentioned, is tightly regulated.
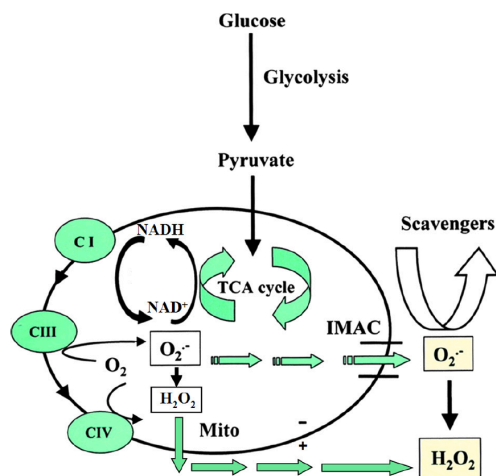
Figure 1.4. Generation of superoxide anion (O_2^-) within the mitochondrial ETC. Adapted and modified from Zorov *et al*.

Oxidative stress is triggered due to an imbalance in the formation of ROS and the subsequent scavenging of ROS. When the amount of ROS generated exceeds the amount of ROS detoxified by intracellular anti-oxidants, the cell enters a state of oxidative stress (118). This can occur either due to a dysregulated production of ROS at the mitochondrial ETC or defects in the function of ROS scavenging enzymes within the cytosol and/or the mitochondrial matrix, or in certain cases, both. When the amount of ROS produced within the mitochondrial matrix exceeds a threshold amount, unique to physiological functioning of the cell, there can be an irreversible opening of the mPTP (119) (Figure 5). In steady state, this pore within the inner mitochondrial membrane switches rapidly between a close to an open to a close state again, maintaining mitochondrial membrane potential and allowing transfer of essential molecules across the mitochondrial membrane (119). Under conditions of dysregulated

ROS production, increase in levels of ROS is accompanied by a fall in the

mitochondrial membrane potential and subsequent opening of the mPTP (120,

121) (Figure 5). The latter is an irreversible signal for unhealthy mitochondria to

either trigger apoptosis by disintegration of the ETC and release of Cytochorome

c into the cytosol, or be cleared by autophagic proteins interacting with signals

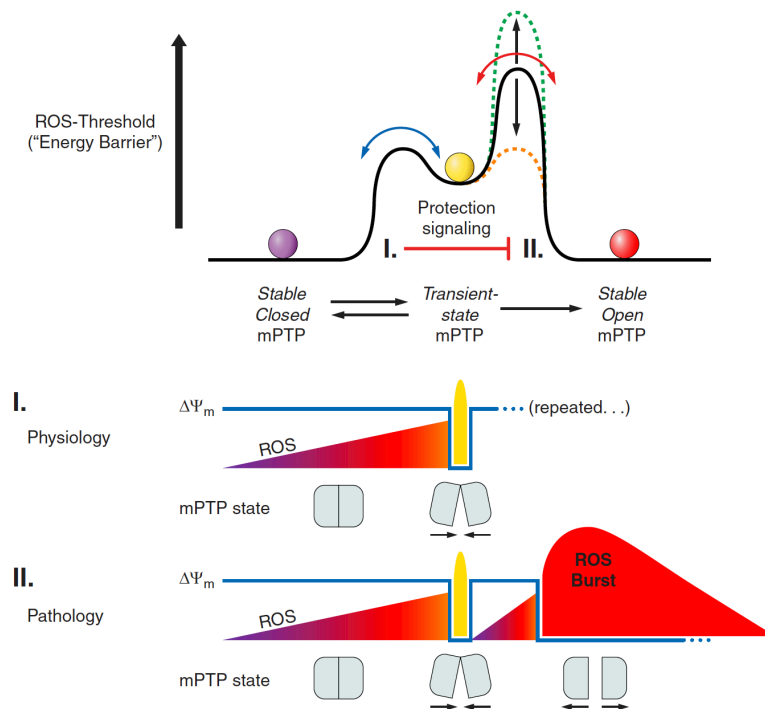triggered through high levels of ROS in order to maintain cellular viability (122,

123, 124).

Figure 1.5. ROS and opening of mitochondrial permeability transition pore. Adapted from Zorov *et al*.

ROS in inflammation

While the injurious reactivity of radical oxidants is a threat to cell viability and can trigger cell death, ROS has also recently been implicated in acting as signaling factors contributing to certain cellular functions. It has been proposed that ROS can interact with "ROS receptors" such as the KEAP1-NRF2 complex which plays a role in maintaining oxidative homeostasis by regulating expression of endogenous antioxidants, among other molecule (125, 126). In addition to this, ROS upregulated in the context of infection through PAMP activated TLRs has also been shown to upregulate cytokines such as IL6 by inhibition of negative regulators such as proteases that cleave MAP kinases (127, 128). Alternatively, there is also evidence to implicate ROS in the IL1-β mediated activation of the NLRP3 inflammasome (129, 130). Moreover, further implications of crosstalk between ROS and cytokines comes from recent evidence suggesting that TNFα mediated activation of the TNF receptor pathway can also upregulate mitochondrial ROS (131, 132, 133). While there is some contradictory evidence of ROS being able to activate NF-κB in specific circumstances, the generally accepted consensus is that TNF mediated upregulation of ROS can deactivate NF-κB as an intrinsic regulatory mechanism for shutting down intracellular processes as part of programmed cell death (134, 135).

Cell Death

Multiple metabolic cues can converge within a cell to orchestrate programmed cell death in order to meet demands of broader physiological

functions involved in embryogenesis and elimination of cells injured beyond

possibility of repair, among others. Apoptosis is the most well characterized form

of programmed cell death mediated by cysteine proteases called caspases. In

steady state, the two major types of caspases- initiator caspases and effector

caspases reside within the cytoplasm (136). Cell intrinsic apoptosis is primarily

triggered by pro apoptotic factors residing within the mitochondria (124).

Upregulation of ROS, depolarization of mitochondrial membrane and irreversible

opening of the mPTP releases components of the ETC into the cytosol, including

cytochrome c (122, 123). Released cytochrome c then works through a series of

coordinated steps to activate initiator caspases like caspase 9 that in turn go on

to activate effector caspases 3 and 7 in a domino effect (137, 138). Effector

caspases are capable of cleaving multiple cellular proteins as part of the

apoptotic machinery. It is also worthwhile to note that apoptosis can also be

executed in a mitochondria independent cell extrinsic process through activation

of caspase 8 (139, 140).

Although apoptosis is considered to be the most evolutionarily conserved

form of programmed cell death, there are certain other non-apoptotic forms of

cell death that can work independently or in line with apoptosis for cell killing

(Figure 6). One such non-apoptotic form of cell death is Necroptosis (141). While

TNFα mediated activation of the TNFR is the primary activator of Necroptosis,

TL3 or TLR4 stimulation has also been implicated this process (142, 143, 144,

145, 146). Activation of these signaling pathways ultimately lead to the

deubiquitylation of a proteins kinase called RIPK1 allowing it to interact with

another kinase called RIPK3 to generate a complex called the Necrosome (147, 148). This, on one hand can activate ROS production by the mitochondria and on the other hand can induce cellular swelling or oncosis and rupture of the plasma membrane mediated by the phosphorylated and oligomerized form of the pseudokinase MLKL (149, 150). Another form of non-apoptotic cell death is pyroptosis. This type of cell death is mainly reliant on cytokines such as IL-1α and IL-1β in a caspase 1 mediated process that ultimately leads to cell lysis as seen in Necroptosis (151).

Although cell death is one viable option to eliminate damaged cells, in certain circumstances, killing of the cell can be circumvented by targeting damaged organelles or cellular components to intracellular structures for degradation. This process is known as autophagy (152). The general mechanism of autophagy involves damaged cellular components to be targeted to double membrane bound autophagosomes which can then fuse with lysomes to induce degradation through the action of lysosomal hydrolases (153, 154). There are many proteins highly conserved across mammals that constitute the autophagy machinery, including Beclin-1 which initiates the process and Atg8 or LC3 which is required to be inserted into the autophagosome membrane required for expansion of the autophagosome to encapsulate intracellular components and its subsequent fusion with lysosomes (155, 156). This process of autophagic removal of damaged molecules can be regulated by multiple factors, including mitochondrial generation of ROS. Both superoxide anion (O_2^{-}) and hydrogen

peroxide (H_2O_2) have been implicated in triggering autophagy (157, 158, 159).

However, recent evidence also reveals a mutually suppressive role of

mitochondrial ROS mediated activation of apoptosis, and initiation of autophagy,

with the latter suppressing factors within the mitochondria to inhibit apoptosis.

Indeed, it has been shown that suppression of autophagy can upregulate

mitochondrial ROS levels with a concurrent depolarization of the mitochondrial

membrane, a release of cytochrome c into the cytosol and activation of apoptosis

(160, 161).
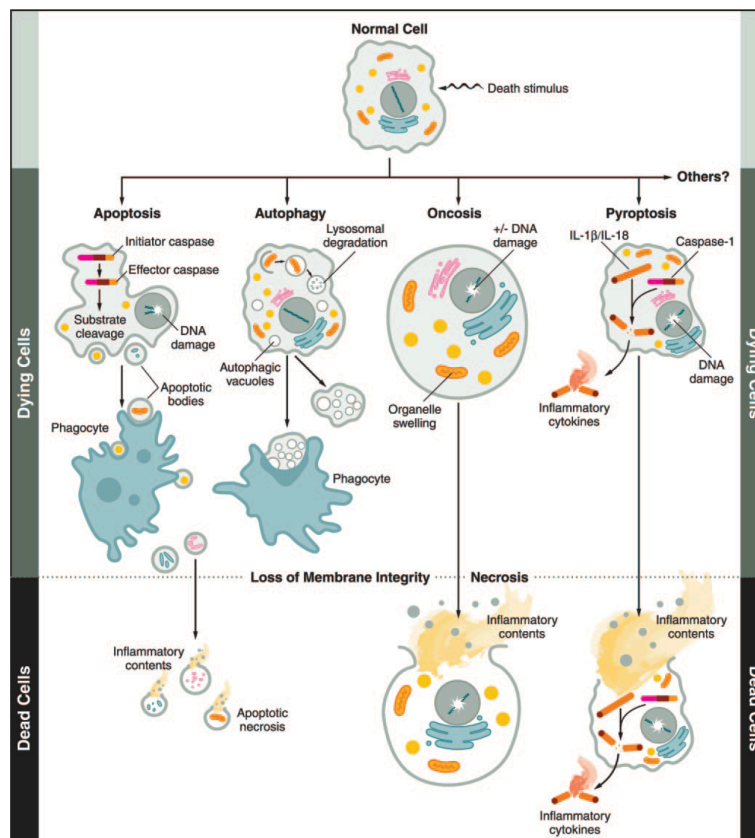
Figure 1.6. Intrinsic cellular processes triggered in response to cellular injury. Adapted from Fink and Cookson *et al.*

Anemia of Inflammation

Diseases and evolutionary rationale

A majority of microorganisms, including many pathogens require iron as an essential element for biological processes. They require iron as an essential component of enzymes participating in oxidative phosphorylation, DNA replication, to maintain overall cellular morphology, in production of toxins and other processes. Their iron requirement in certain cases exceeds their available iron stores, therefore many pathogens have elegant mechanisms to acquire iron from host sources. Sometimes this iron availability from host sources allows an opportunistic pathogen to establish infection and damage host cells (162, 163, 164). As a result of this, host iron stores and availability are tightly linked to disease susceptibility, onset of infection and subsequent prognosis. Patients with hereditary hemochromatosis (iron overload), high iron levels due to repeated blood transfusions, or medical regimens that include high levels of oral or parental iron supplementation, as well as consumption of iron rich diets have been found to be susceptible to acute infections by pathogens such as *Vibirio*

vulnificus, Yersinia enterolitica, Yersinia pestis, etc (165, 166, 167).

Pathophysiology of many chronic inflammatory conditions including kidney

disease, diabetes, neurodegeneration, inflammatory bowel disorder, rheumatoid

arthritis, etc has also been linked to high levels of iron in the body (5, 10, 11).

This link between iron loading and inflammation, whether acute or chronic,

underlies the evolution of AI (also known as Anemia of Chronic disease), wherein

the body adapts to an iron deficient state to ameliorate inflammation and resist

infection by pathogens.

Primary mechanism and signaling pathway

Many bacterial infections release ligands TLRs for example

lipopolysaccharide-a TLR4 ligand. Activation of the TLR pathway results in an

NFκB mediated production of inflammatory mediators, including the pro

inflammatory cytokine IL6 that has been implicated in causing anemia by

upregulating Hepcidin (168, 169, 170, 171, 172). IL6 treatment in cultured

Hepatocytes and HepG2/2.2.1 cells upregulated Hepcidin mRNA expression. IL6

binding to the IL6 receptor triggers activation of the JAK-STAT pathway. STAT3

is phosphorylated and becomes capable of translocating to the nucleus and

binding to the hepcidin promoter, inducing hepcidin expression (Figure 7). In

HepG2/2.2.1 cells treated with IL6, chromatin immunoprecipitation studies

revealed binding of STAT3 to the Hepcidin promoter (172).
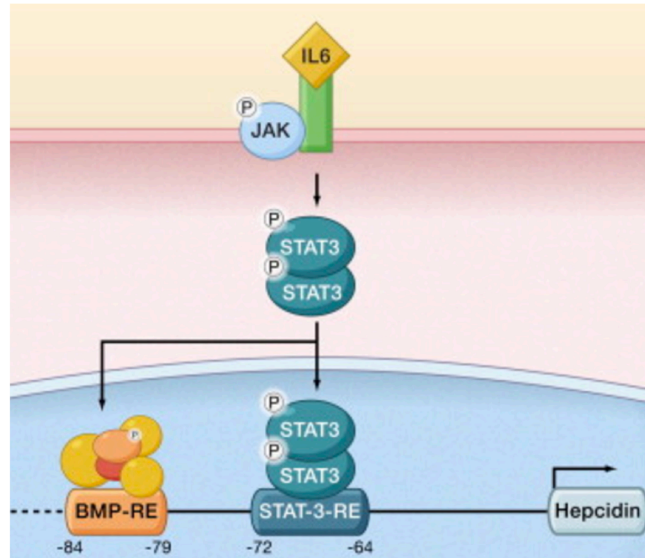
Figure 1.7. IL6 activation stimulates the Hepcidin promoter. Adapted from Hentze *et al*.

Hepcidin in turn causes hypoferremia by preventing iron export through the internalization and degradation of Ferroportin (described previously in this chapter). Degradation of Ferroportin leads to an intracellular retention of iron within cells such as macrophages and a concurrent fall in iron availability for erythroid progenitor generation. Thus, a state of IRE ensues, with high levels of iron entrapped in the reticuloendothelial system -both of which are classic hallmarks of anemia of inflammation. In contrast with a normal state of iron absorption, IRE is characterized by low plasma iron but elevated iron accumulation within cells such as macrophages (173, 174). (Figure 8). Additionally, it has also been suggested that inflammation independent STAT3 activation can also induce Hepcidin expression and regulate iron availability, further underscoring the importance of this pathway as the primary cause of

anemia in anemia of inflammation (172). Although Hepcidin is upregulated

immediately following administration of an inflammatory insult, in an

erythropoietic stimulation model of AI in mice, it was found that under conditions

of anemia, serum hepcidin levels begin to decline as early as 14 days following

erythropoietic stimulation (175). This indicates a potential generation of iron

overload conditions at later time points, giving rise to the possibility of NTBI

mediated damage in AI.
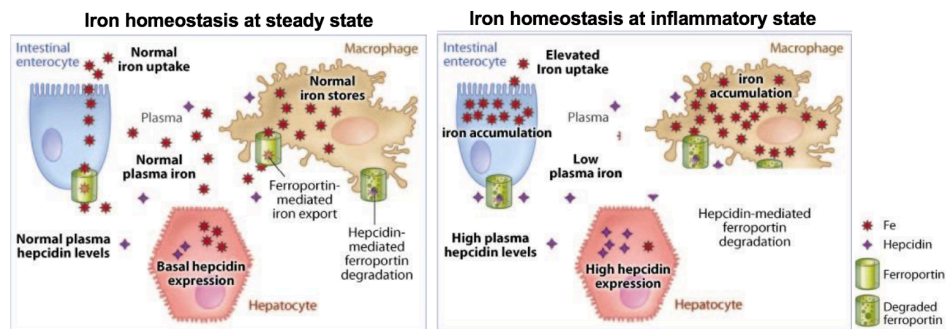
Figure 1.8. Hallmarks of IRE induced by changes in iron homeostasis under inflammation. Adapted and modified from Lee *et al*.

Additional causes of anemia of inflammation

Another cytokine implicated in IRE is IL1. Primary murine hepatocytes

from IL6$^{-/-}$ mice were capable of inducing Hepcidin expression, and only failed to

induce Hepcidin in the presence of blocking antibodies for IL1-α, IL1β and IL6

(176). IL1 induces Hepcidin expression through C/EBPα, a transcriptional

regulator of Hepcidin (177, 178). This transcription factor also has independent

contributions to anemia of inflammation through the ER stress pathway. Cellular

damage can trigger activation of the ER unfolded protein response. ER stress

response proteins can downregulate expression of CHOP, which is a negative

regulator of C/EBPα. Relieving repression of C/EBPα contributes to Hepcidin

expression and subsequent anemia (179, 180, 181).

HMGB1, a cytokine mediator of inflammation produced by cells such as

macrophages, is capable of binding to the MD-2-TLR4 complex, resulting in

NFκB mediated production of cytokines like IL6 that cause IRE (182, 183). TLR2

and TLR4 can also induce iron sequestration and IRE in a hepcidin independent

manner. TLR pathways can trigger the production of Lipocalin-2 by

macrophages. Lipocalin is an acute phase protein implicated in iron

sequestration (184, 185). Another acute phase protein is Ferritin. In steady state,

Ferritin is an intracellular protein, and apoferritin binds to ferrous iron and stores

it as ferric iron within cells, including those of the reticuloendothelial system

(186). Although small amounts of Ferritin are secreted in steady state, under

inflammatory conditions, levels of extracellular plasma ferritin increase and can

be used as an indicator of inflammation (187, 188, 189). Whether this ferritin can

extracellularly bind to iron from a labile iron pool in the serum remains to be

seen. Additionally, inflammatory TLR mediated stimulation of neutrophils can

result in the production of Lactoferrin, a homolog of Tf which unlike Tf does not

release Iron in the low pH of the endosomal system, contributing to yet another

arm of iron sequestration in the face of infection (190). Inflammatory mediators

can also contribute to the production of Nramp-1, a phagosomal transporter that

sequesters iron and prevents its acquisition by invading pathogens (191, 192).

Multiple erythropoiesis associated genes involved in the anemia of inflammation

response including Nramp1, ferroportin, DMT1, TfR1 and erythropoietin are also

regulated by the family of HIFs (Hypoxia inducible factors), and in turn HIF1-α is

transcriptionally controlled by NFκB thereby linking the inflammatory signaling

pathways to a HIF mediated regulation of iron homeostasis (193, 194).

Mouse models of anemia of inflammation

While in vitro culture systems can be used to study some features of AI,

the mouse physiological system, due to its close similarity to humans has been

adapted as an ideal model for investigation into various aspects of AI. There are

other mammalian and non- mammalian models also available for studying AI, but

due to its relative ease of handling, reproducibility, and extensive erythropoietic

response mimicking that of humans, the mouse model remains the most

preferred one.

Non-infectious mouse models of AI include injection of Turpentine and

models imitating autoimmune conditions such as collagen induced arthritis for

examining certain features of rheumatoid arthritis and an oral administration of

dextran sulfate sodium to model inflammatory bowel disease. While these

models do induce significant anemia, increased Hepcidin expression is not

always maintained (195, 196, 197, 198). Moreover, results are often unique to

the type of disease under investigation, and might not be an accurate

representation of acute inflammatory conditions.

Certain infectious models are also in practice for studying AI. These include CLP and introduction of catheters or dextran microbeads coated with bacteria such as *Staphylococcus epidermidis*, *Staphylococcus pyogenes*, *Staphylococcus aureus*. These mice do develop mild but significant anemia, although not always associated maintenance of elevated Hepcidin levels. There are however technical difficulties often associated with CLP, and higher morbidity, which has since limited the use of this model for studying AI (199, 200).

Currently, pseudo-infectious models are the most extensively studied models for investigating AI. These involve the use of immunogenic particles derived from infectious organisms that are able to mimic the inflammatory response in a disease setting to a certain extent and also simultaneously display hallmarks of IRE. A single IP injection of CFA was able to induce iron restricted anemia characterized by drop in hemoglobin and MCV levels. Injection of lipopolysaccharide has also been demonstrated to cause anemia in mice (201, 202, 203).

A recent and effective pseudo-infectious mouse model to study AI involves a single IP injection of the *Brucella* ring test antigen consisting of heat-killed particles of the gram-negative bacterium *Brucella abortus*. Two weeks after injection of BA, WT mice show the lowest level of hemoglobin, a significant drop

by 5-6 g/dL in comparison to controls (205). This anemia is iron restricted and more severe in comparison to the other mouse models discussed previously. Anemia is also accompanied by a rise in serum Hepcidin and a concurrent fall in serum iron levels as early as 6 hours after injection of BA. Although IRE is the primary cause of hypoferremia in this model, the kinetics of drop in hemoglobin so early in the response also suggest possible RBC hemolysis contributing to anemia (173, 204, 205, 206, 207, 208).

Existing information on the contribution of IL6 in AI

Existing literature and previous work by us elucidates the significance of IL6 and Hepcidin in AI. In both the *IL6*-KO and *Hamp*-KO mice injected with BA, recovery was found to be improved in terms of CBC parameters, in comparison to WT controls. However, the *IL6*-KO mice showed improved erythropoiesis in the BM a week after BA administration, in comparison to iron overloaded *Hamp*-KO mice (173) (Figure 9). On observing these differing modes of recovery in *IL6*-KO and *Hamp*-KO mice, we wanted to further study the cellular responses governing erythroid recovery in the absence of IL6 under inflammatory insult, and additionally, the influence of iron and iron overloading conditions on BM erythropoiesis under the same. The results of our study are described in the next chapter.
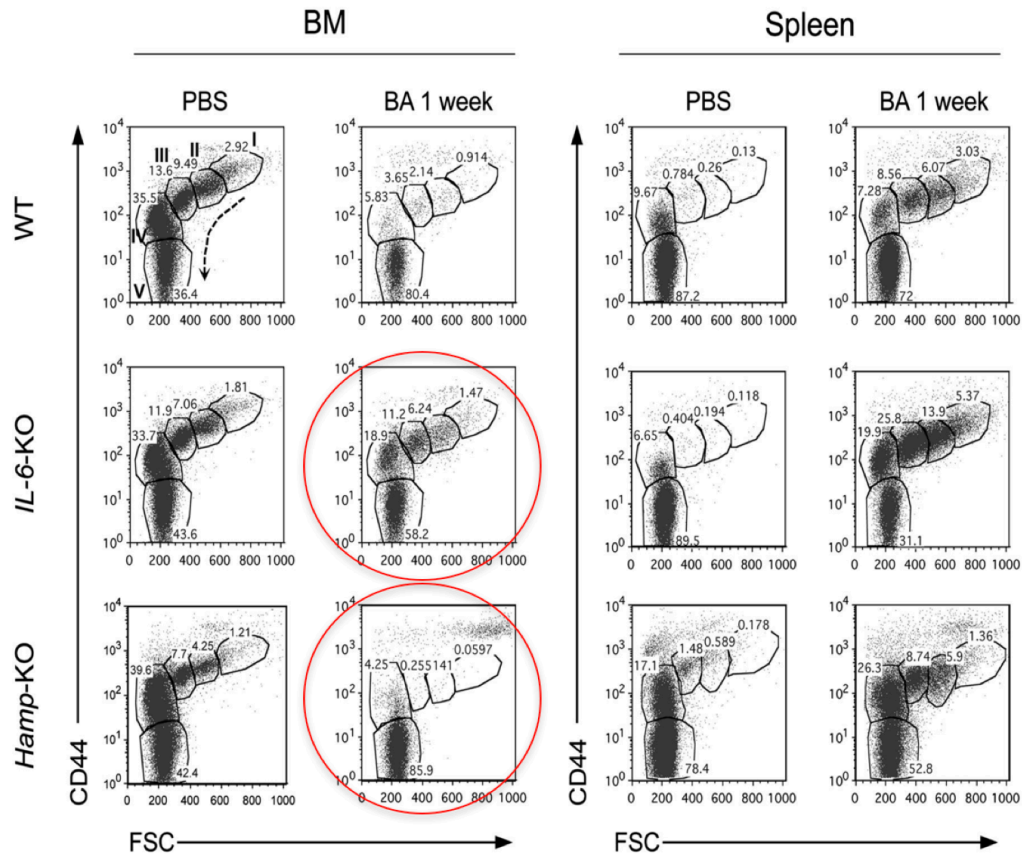
Figure 1.9. IL6 KO mice show improved BM erythropoiesis under AI.
Adapted from Gardenghi *et al*.

Chapter Two

Results: Lack of IL6 protects erythroid recovery under AI, a process reversible by iron dependent ROS upregulation

Summary: In our study, we show that under inflammatory insult, terminal erythroid differentiation within the BM is improved in the absence of IL6. We further demonstrate that this lack of IL6 mediated protective effect is lost in conditions of iron overload, by a ROS dependent detrimental effect on BM erythropoiesis.

The IL6-KO mice showed improved BM erythropoiesis two weeks after BA administration with a concurrent regression in BM erythroid recovery of the DKO

Considering existing information on the different patterns of erythroid recovery in *IL6*-KO and the iron overloaded *Hamp*-KO, we generated a DKO of IL6 and Hamp, to investigate potential independent roles of the two genes in AI and furthermore, to study BM erythropoiesis of the *IL6*-KO in the context of iron overloading. The *IL6*-KO, *Hamp*-KO and DKO showed an improved erythroid recovery in comparison to the WT (Fig 1A, B, C, D). Despite this improved recovery, both iron overloaded models (the DKO and the *Hamp*-KO) showed similar hemoglobin levels, MCV, MCH and RBC (Fig 1A, B, C, D).
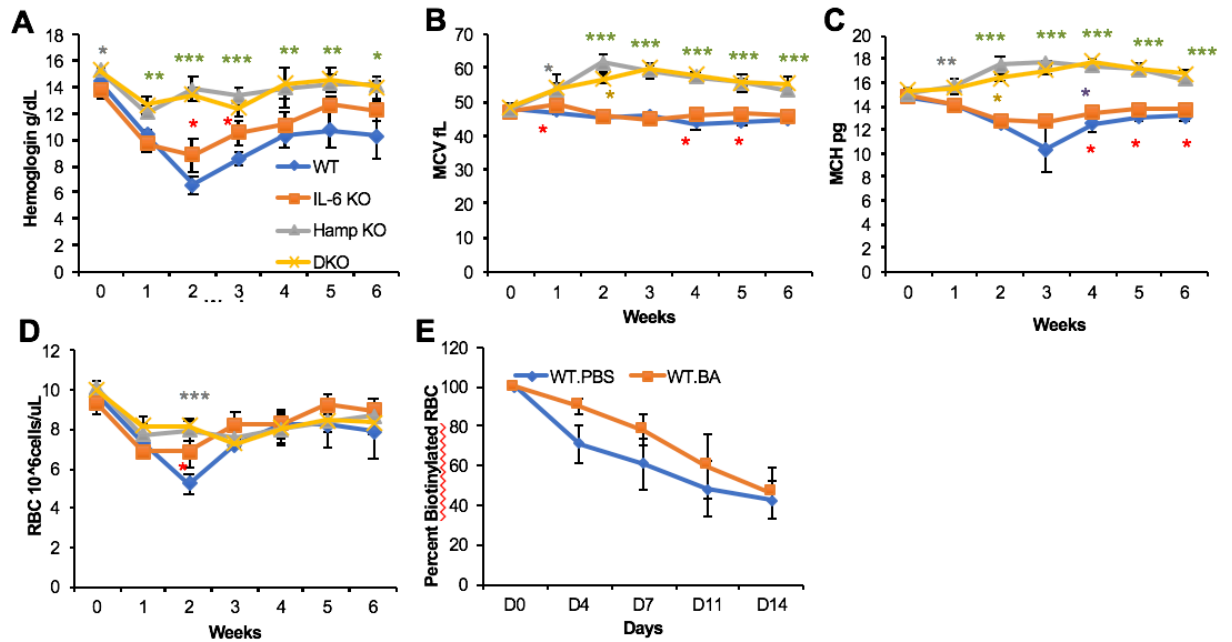
Figure 2.1. Both iron overloaded models of *Hamp*- KO and the DKO show similar recovery of peripheral blood hemoglobin levels under AI. * P< 0.05, ** P <0.01, *** P < 0.001. (A) Hemoglobin levels in peripheral blood of WT, *IL6*-KO, *Hamp*-KO and DKO mice. Peripheral blood was collected at 0, 1, 2, 3, 4, 5, and 6 weeks after injection of BA (Mean±SD, n=15, results are representative of two independent experiments). (B) As in (A), but for MCV (mean corpuscular volume) levels. (C) As in (A), but for MCH (mean corpuscular hemoglobin) levels. (D) As in (A), but for RBC levels. (E) Percentage of biotinylated RBC in peripheral blood of WT mice injected with biotin and injected with BA, as measured by flow cytometric analysis of peripheral blood. Biotinylated RBC measurement was done at 0, 4, 7, 11 and 14 days after injection of BA (Mean±SD, n=5, statistics are in comparison with PBS injected control mice).

The DKO however, solely showed a biphasic effect in reticulocyte count, with numbers that peaked one week after BA administration, and then dropped on the second week (Fig 2A). To confirm this initial rise in peripheral blood count and subsequent fall, we measured RBC lifespan at similar time points-one and two weeks after BA injection. Unlike RBC life span in the WT injected with BA (Fig 1E), the *IL6*-KO, *Hamp*-KO and the DKO all show a decrease in production of biotinylated RBCs on BA injection, indicating production of new "non-

biotinylated" RBCs in response to the anemia (Fig 2B, C, D). However, the DKO

shows the drop in biotinylated RBCs one week following BA administration,

indicating an accelerated production of new RBCs in comparison to the *IL6*-KO

and the *Hamp*-KO where the drop occurs 11 days after BA administration. (Fig

2B, C, D). This accelerated production of new RBCs in the DKO (Fig 1B) occurs

at the same time as the rise in its reticulocyte count (Fig 2A). Furthermore,

although the percentage of biotinylated RBCs initially continues to decrease upon

BA administration, this decrease pauses after day 11 and the curve plateaus 2

weeks after BA administration (Fig 2B) indicating a potential suspension in the

generation of new RBCs. This time point also coincides with the fall in

reticulocyte count of the DKO, seen two weeks following inflammatory insult (Fig
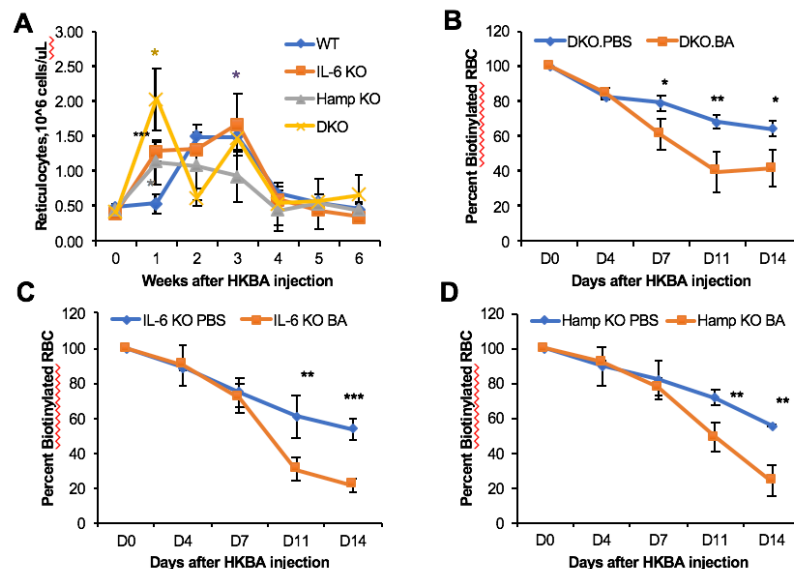
2A).

Figure 2.2. The DKO displays a biphasic trend in peripheral blood cell count. * P< 0.05, ** P <0.01, *** P < 0.001 (A) As in Figure1A, but for reticulocyte count. (B) Percentage of biotinylated RBC in peripheral blood of DKO mice

injected with biotin and injected with BA, as measured by flow cytometric analysis of peripheral blood. Biotinylated RBC measurement was done at 0, 4, 7, 11 and 14 days after injection of BA (Mean$\pm$SD, n=5, statistics are in comparison with PBS injected control mice). (C) As in (B), but in *IL6*-KO mice. (D) As in (B) but in *Hamp*-KO mice.

Following our study on peripheral blood count, we assessed BM terminal

erythroid differentiation of all four genotypes after BA injection, to confirm

maintenance of a biphasic effect in the DKO. Immediately following inflammatory

insult, when we looked at BM erythropoiesis 3 days after injection of BA, we

found that the WT, Hamp-KO, IL6-KO and the DKO showed a drastic reduction in

erythroid progenitor differentiation in response to the inflammation (Figure 3A).

Early in the response to BA, all four genotypes were equally affected in BM

erythropoiesis. However, one week after administration of BA, we find that the

IL6-KO, *Hamp*-KO and the DKO began to show an improvement in BM erythroid

progenitor differentiation, in comparison to the WT. (Fig 3B). Nonetheless at this

time point, the DKO shows the highest improvement in terminal erythroid

differentiation, with the maximum expansion of erythroid progenitor populations in

comparison to the single KOs (Fig 3B). Since, one week following inflammatory

insult we detected an improvement in erythroid progenitor differentiation, we

quantified the absolute cell numbers of each progenitor population at this time

point and further confirmed the improved BM terminal erythroid differentiation of

the DKO (Fig 4A). In agreement with the biphasic effect seen previously, this

improved erythroid recovery in the DKO regressed, and the *IL6* KO showed the

most improved BM erythroid differentiation two weeks after administration of BA

(Fig 3C). This significant improvement of BM erythropoiesis following

inflammatory insult in the *IL6*-KO was quantified and confirmed by absolute cell

numbers of the progenitor populations (Fig 4B).
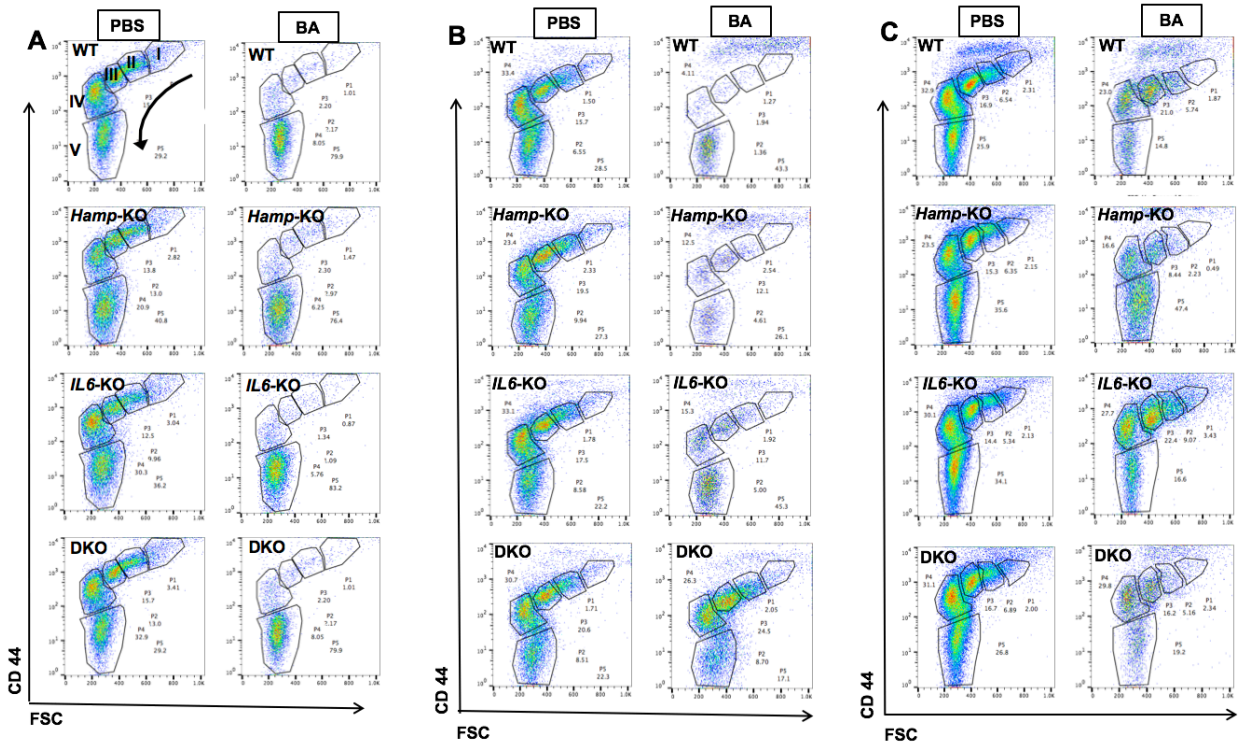
Figure 2.3. Two weeks following inflammatory insult, the *IL6*-KO shows the most improved Bone Marrow (BM) erythroid recovery with a concurrent regression in the same of the DKO. (A) Flow cytometric analysis of BM in WT, *Hamp*-KO, *IL6*-KO and DKO; 72 hours after injection with BA. CD71 (Transferrin receptor), TER119 (erythroid specific) and CD44 (adhesion molecule that progressively decreases in expression from pro-erythroblast to reticulocyte stage) were used. TER119$^+$CD71$^+$ and TER119$^+$CD71$^-$ cells (Erythroid precursors and mature RBCs respectively-not shown here) were selected and plotted as CD44 versus FSC, to show the different stages of terminal erythroid differentiation. Differentiation occurs as indicated by the direction of the arrow, and includes (I) pro-erythroblast, (II) basophilic erythroblast, (III) polychromatic erythroblast, (IV) Orthochromatic and reticulocyte, and (V) mature RBCs. (B) As in (A) but showing flow cytometric analysis of BM in WT, *Hamp*-KO, *IL6*-KO and DKO; one week after injection with BA. (C) As in (A) but two weeks after injection with BA.
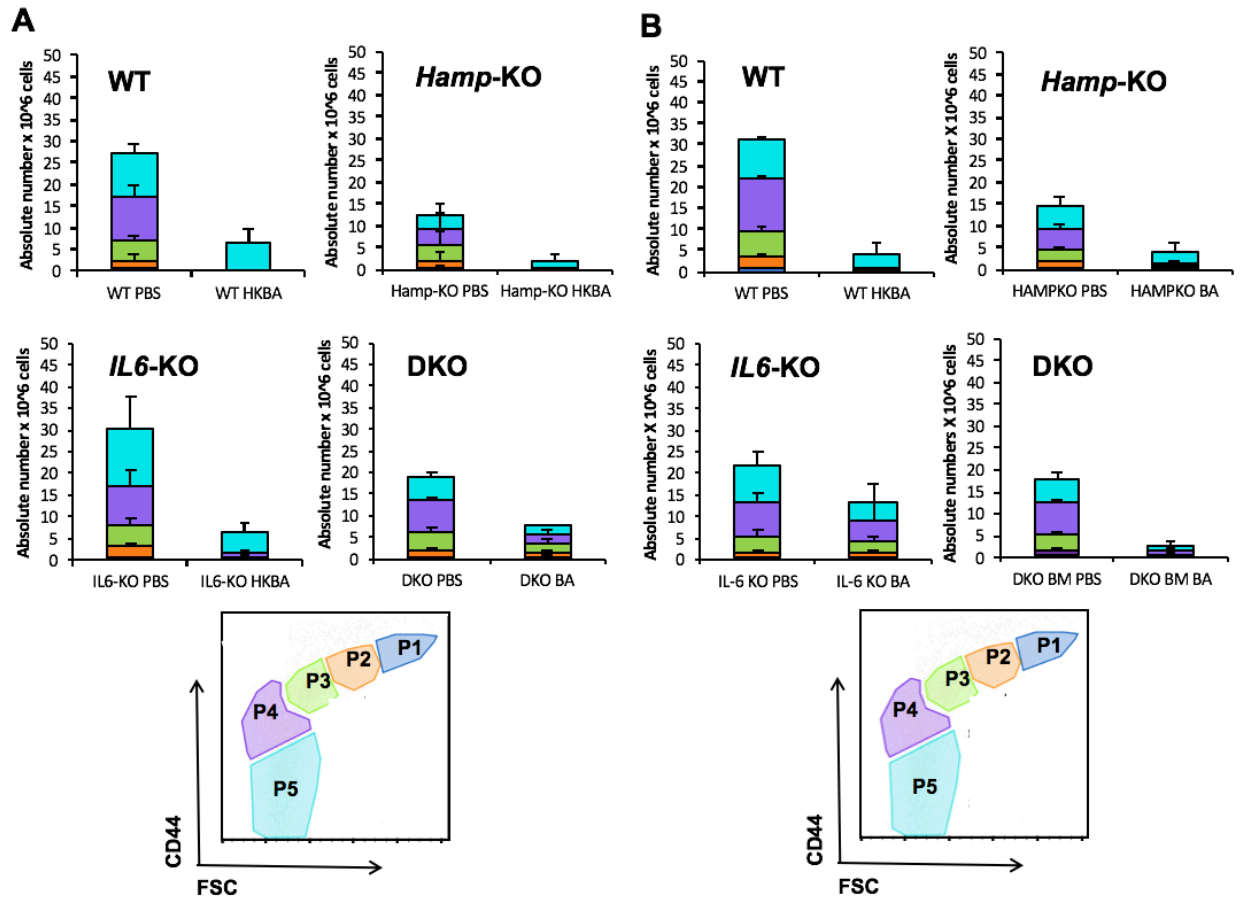
Figure 2.4. Quantification of progenitor cell numbers in the BM confirm improved erythroid recovery of the IL6-KO. (A) Quantification of the flow cytometric dot plots in Fig 3B. Absolute number of cells for each erythroid population (color coded and labelled as P1, P2, P3, P4 and P5, in the flow cytometric dot plot legend) were plotted as bar graphs with each color in the bar graph corresponding to the matching color and population in the flow cytometric dot plot legend. Bar graphs representing PBS injected (Left bar) and BA injected (right bar) in WT, *Hamp*-KO, *IL6*-KO and DKO mice are shown. (B) Quantification of the flow cytometric dot plots in Fig 3C, quantified as in Fig 4A.

Furthermore, the spleen of all genotypes showed extra medullary erythropoiesis one and two weeks following BA administration, with no difference in splenic expansion of erythroid progenitor populations within the *IL6*-KO, *Hamp*-KO and DKO (Fig 5A, B). Interestingly, this phenomenon is then organ specific, as only the BM is affected and not the spleen.
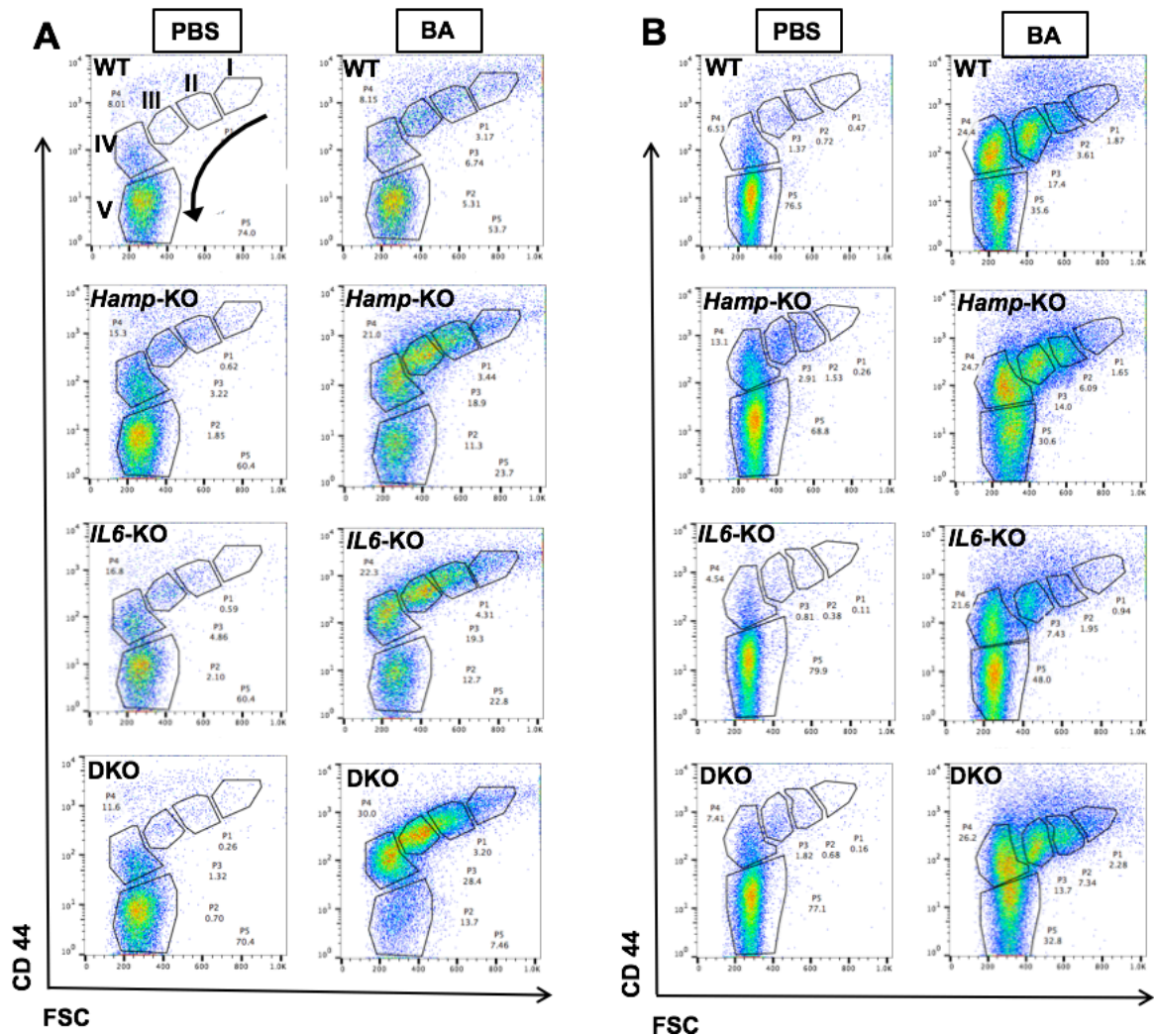
Figure 2.5. The spleen shows no significant difference in extra medullary erythropoiesis, between the Hamp-KO, IL6-KO and the DKO. Flow cytometric analysis of Spleen in WT, *Hamp*-KO, *IL6*-KO and DKO; one week after injection with BA. Terminal erythroid differentiation is analyzed by flow cytometry as described in Figure 3. n=5, each flow cytometric dot plot is representative of one animal per group. (B) As in (A) but two weeks after injection with BA.

Based on the above trend in erythroid recovery that we noted in all four genotypes, we found two major phases of BM erythroid recovery under inflammation in a schematic representation of changes in BM erythroid progenitor cell numbers over time (Fig 6). The first phase is seen immediately following BA

administration. This phase, which been studied previously in literature by others

and by us, is characterized by an upregulation of cytokines and severely reduced

terminal erythroid differentiation in the BM of all genotypes (Fig 6, Fig 3A).

Although the cytokine response and erythroid parameters in the first phase have

been elucidated before, we were able to identify a second phase of BM erythroid

response under inflammation. This second phase is characterized by a

regression in erythroid recovery of the DKO and a concurrent improved recovery

of the *IL6*-KO (Fig 6, Fig 3C). At this phase, the WT and the *Hamp*-KO continue

to show a slackened BM erythropoiesis in response to the inflammation.
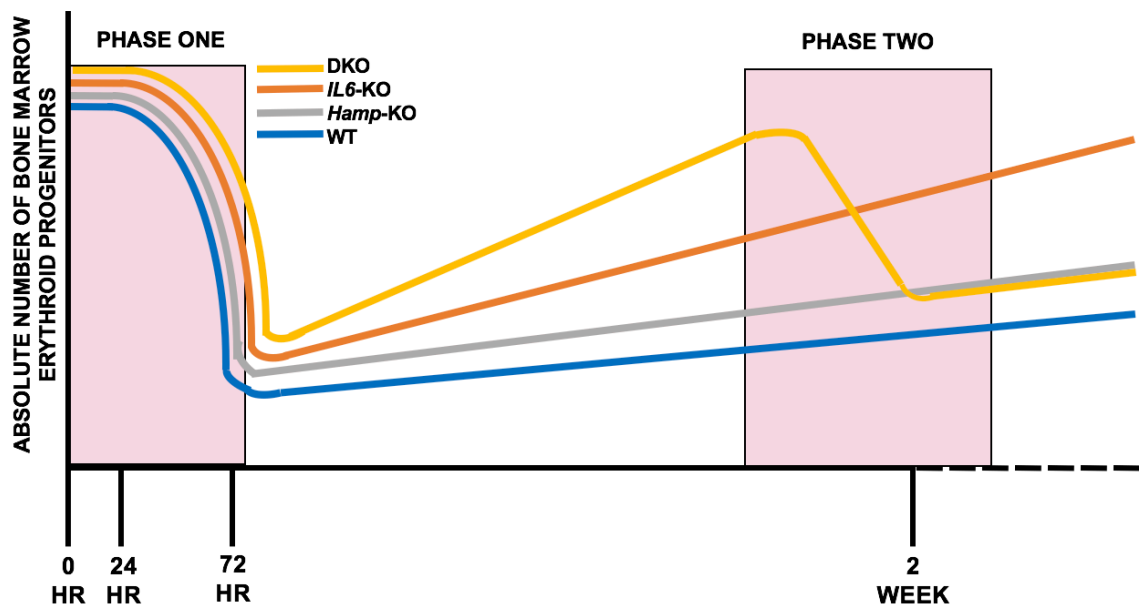
Figure 2.6. Pattern of BM erythroid recovery in the different genotypes reveals two major phases of divergence, phase one and phase two. Schematic representation of changes in numbers of BM erythroid progenitor populations (indicated by the different lines) in the WT, *IL6*-KO, *Hamp*-KO and DKO at different time points following BA injection.

In phase one of recovery under AI, both the WT and IL6-KO show an increase in levels of mitochondrial SO within BM erythroid progenitors

Given the extensive evidence supporting crosstalk between ROS and iron homeostasis, in order to investigate cellular responses contributing to BM erythroid recovery under AI, we looked at changes in ROS generation in the two different phases of recovery following BA administration. As shown previously, we found an expected fall in terminal erythroid differentiation within the BM of WT and *IL6*-KO mice, 72 hours after injection of BA, in the first phase (Fig 7A, Fig 3A). This initial blunted erythropoietic response is also accompanied by upregulated cytokine levels, noted previously by others and by us (Fig 8). We found that this fall in terminal erythroid differentiation following BA administration in both the WT and the *IL6*-KO was preceded by an increase in levels of mitochondrial SO, 24 hours after BA injection, in both the WT and the *IL6*-KO (Fig 7B).

Figure 2.7. During phase one of recovery under inflammation, mitochondrial superoxide levels within BM erythroid progenitors increase in both the WT and the *IL6*-KO. * P<0.05, ** P<0.01, *** P<0.001. (A) Flow cytometric representation of terminal erythroid differentiation (as described in Figure 3), for WT and *IL6* KO mice 3 days after BA injection, n=5. (B) Flow cytometric analysis of mitochondrial superoxide of BM erythroid progenitors in WT and *IL6*-KO mice 24 hours after injection of BA. (from right to left) To select for erythroid progenitors, TER119 (erythroid specific) and CD29 (integrin that progressively decreases in expression from pro-erythroblast to reticulocyte stage and can distinguish between the orthochromatic and reticulocyte stage by difference in expression) were used. TER119+ cells were selected and plotted as CD29 versus FSC and subsequently the pro-erythroblast to orthochromatic stages were selected for analyzing mitochondrial superoxide (SO) expression by histogram. Cells in the histogram were gated into SO positive, indicating cells with high expression of SO (extreme right panel of B.) Histogram of SO expression on cells of these selected erythroid progenitor stages in PBS and BA injected mice is shown, red line indicates PBS injected control and blue line indicates BA injected. Percentage of cells in the SO positive gates were plotted in bar graphs, red bars indicate PBS injected and blue bars indicate BA injected. n=3, histogram of sample from one representative mouse is shown.

42
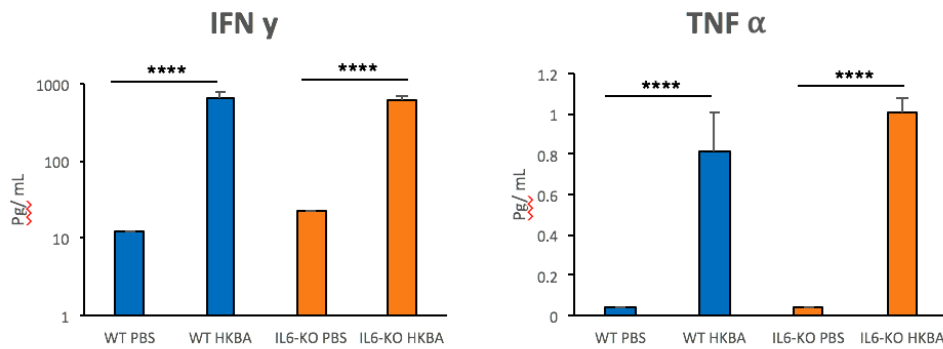
Figure 2.8. In phase one of recovery under inflammation, both WT and *IL6*-KO upregulate serum cytokines. * P<0.05, ** P<0.01, *** P<0.001 (A) IFN y and TNFα cytokine levels in serum of WT and IL6-KO mice 24 hours after injection of BA, in comparison to PBS injected controls were plotted in bar graphs. Blue bars indicate WT and orange bars indicate *IL6*-KO, n=5.

In phase two of recovery under AI, WT erythroid progenitors upregulate expression of ROS, while the IL6 KO does not

Two weeks after BA injection, we identified a second phase of erythroid response to BA which, similar to phase one, was characterized by an upregulation of cytokines IFNy and TNFα in both the WT and the *IL6*-KO mice (Fig 9A). Unlike the response in phase one, under the second phase of recovery under inflammation, the *IL6*-KO showed improved BM erythropoiesis in comparison to the WT, two weeks after injection of BA (Fig 9B, Fig 3C). This divergence in erythroid recovery between the *IL6-KO* and the WT was also preceded by a divergence in mitochondrial SO production by BM erythroid progenitors of the two genotypes, 10 days after injection of BA. We found that, the *IL6*-KO which showed improved erythroid recovery, normalized mitochondrial

43

SO in the second phase, in comparison to the WT which continued to show
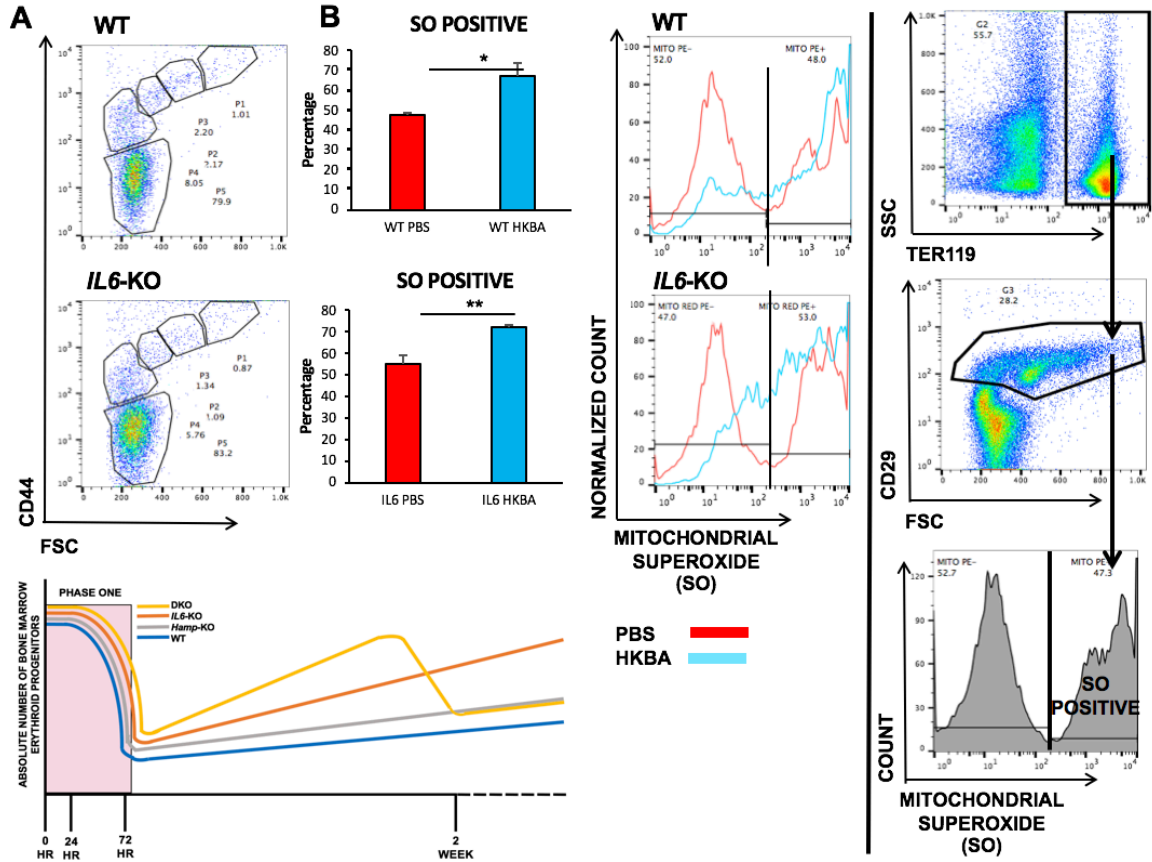
upregulated mitochondrial SO (Fig 9C).

Figure 2.9. During phase two of recovery under inflammation, mitochondrial superoxide levels within BM erythroid progenitors increase in the WT but not in the *IL6*-KO. * P<0.05, ** P<0.01, *** P<0.001 (A) IFN γ and TNFα cytokine levels in serum of WT and IL6-KO mice 2 weeks after injection of BA, in comparison to PBS injected controls were plotted in bar graphs. Blue bars indicate WT and orange bars indicate IL6-KO, n=5 (B) Flow cytometric representation of terminal erythroid differentiation (as described in Figure3), for WT and IL6 KO mice 2 weeks after BA injection. n=9. (C) Flow cytometric analysis of mitochondrial superoxide of BM erythroid progenitors in WT and *IL6*-KO mice 10 days after injection of BA, analyzed as in Figure 7. n=3, histogram of sample from one representative mouse is shown.

This divergent pattern of mitochondrial SO generation between the two

groups in the second phase of recovery under AI prompted us to investigate

ROS generation further in this phase. Two weeks after administration of BA, BM

erythroid progenitors of the WT upregulated expression of cytoplasmic ROS,

while the *IL6*-KO was protected (Fig 10A). Moreover, at the same time, the WT

showed an increase in total protein oxidation of whole BM cells, but the *IL6*-KO

did not (Fig 10B). It is noteworthy that this lack of ROS upregulation in the *IL6*-

KO two weeks after inflammatory insult coincides with an improved BM
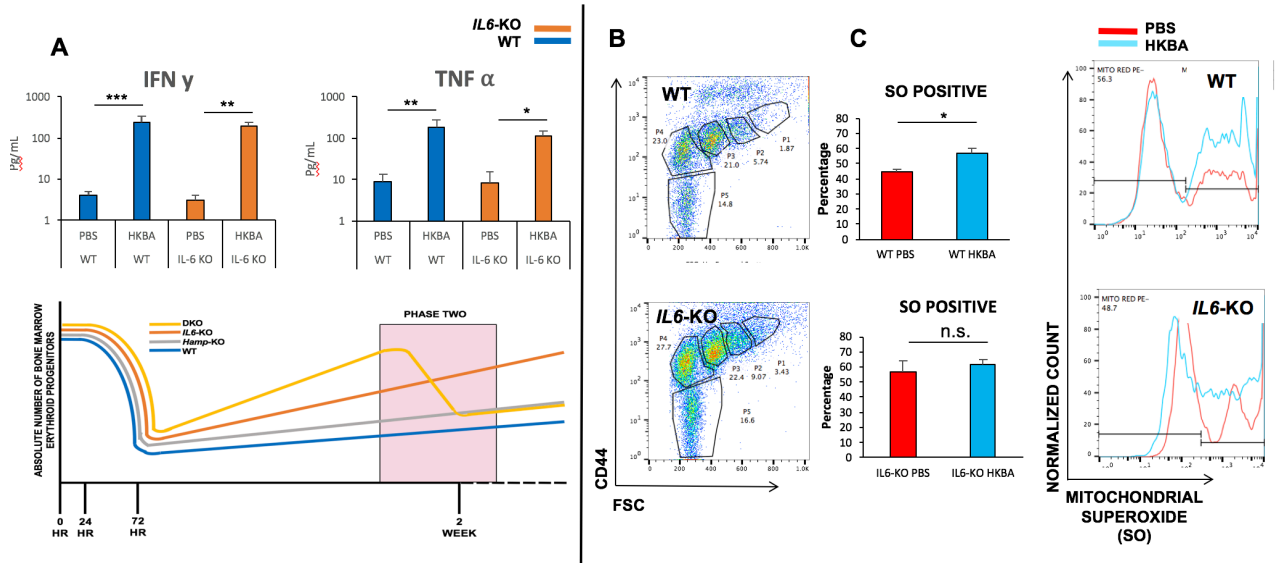
erythropoiesis (Fig 9B, Fig 3C).
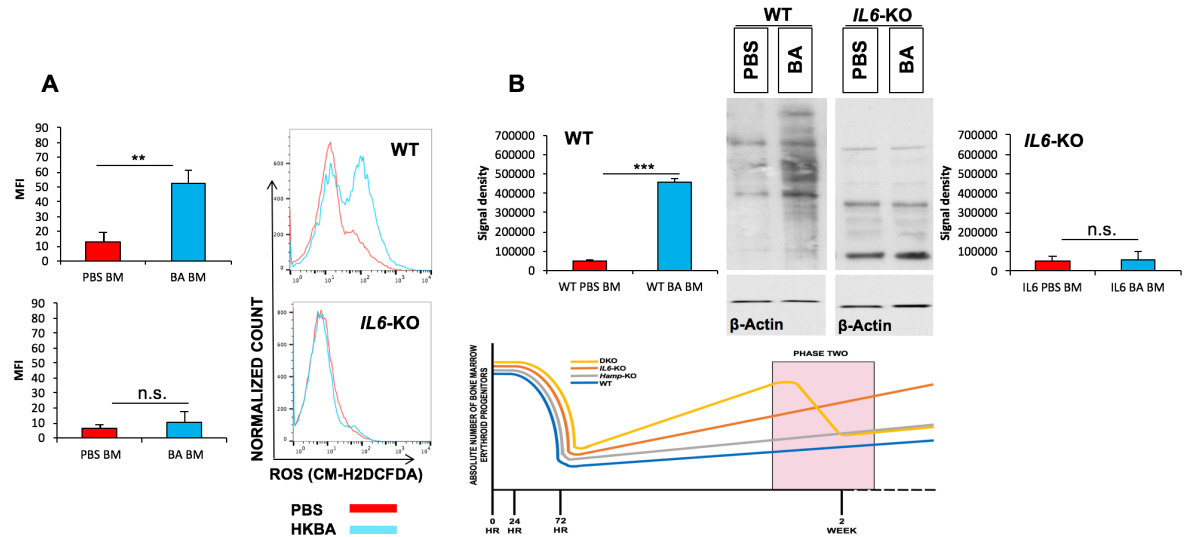
Figure 2.10. During phase two of recovery under inflammation, cytoplasmic ROS levels within BM erythroid progenitors increase in the WT but not in the *IL6*-KO. * P<0.05, ** P<0.01, *** P<0.001 (A) Flow cytometric analysis of cytoplasmic ROS of BM erythroid progenitors two weeks after injection of BA. Eryhthroid progenitors were selected by flow cytometric analysis (as in Figure 7). Cytoplasmic ROS levels in these selected erythroid progenitors is shown by a histogram of the general oxidative indicator CM-H2DCFDA. Red lines indicate PBS injected and blue lines indicate BA injected. n=9, histogram of sample from one representative mouse is shown. The MFI of the histogram were plotted in bar graphs, red bars indicate PBS injected and blue bars indicate BA injected. (B) Oxyblots indicating total protein oxidation of whole BM cells two weeks after injection with BA. n=4, one oxyblot from one representative mouse is shown. Increase in signal of the blot indicates increase in total protein oxidation. Signal density of the oxyblots were quantified into bar graphs by image J; red bar indicates PBS injected and blue bar indicates BA injected.

When we examined erythroid progenitors in the spleen two weeks after

BA administration, we found no change in cytoplasmic ROS expression in splenic

erythroid progenitors of either the WT or the IL6-KO mice (Fig 11A), in

agreement with no defect in erythroid production in this organ. Moreover, upon

BA administration, we found no change in total protein oxidation within the WT

spleen, and a decrease in total protein oxidation in the *IL6*-KO spleen (Fig 11B).
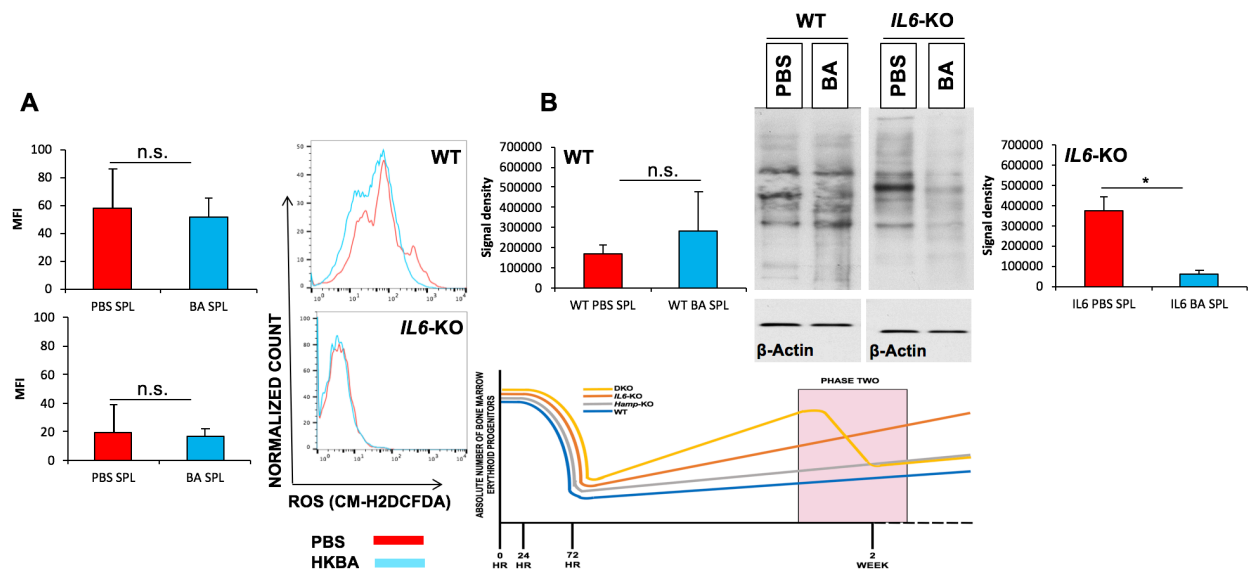
**Figure 2.11. During phase two of recovery under inflammation, the spleen
is protected from ROS upregulation.** (A) As in Fig 10A, but indicating
cytoplasmic ROS levels in splenic erythroid progenitors, two weeks after injection
of BA, n=9. (B) As in Fig 10B, but indicating total protein oxidation of whole
spleen cells two weeks after injection of BA, n=4.

Improved BM erythropoiesis of the IL6 KO under inflammation is

reversible in the presence of iron

We postulated that ROS upregulation is potentially a physiological by

product of stress erythropoiesis and not necessarily detrimental to erythroid

recovery. However, upregulated ROS can impair erythroid recovery in the

presence of high levels of iron. We further hypothesized that although lack of IL6

is protective in phase two of response, lack of IL6 in combination with conditions

of iron overload exacerbates the latter's effect on impeding terminal erythroid

differentiation in the BM. In line with our hypothesis, we found that in WT mice

phlebotomized to induce acute stress erythropoiesis, ROS was upregulated in

BM erythroid progenitors (Fig 12A). Since erythropoiesis under stress is not

impaired, but rather shows an expansion of the erythroid progenitor pool to meet

demands of erythrocyte generation, this upregulation of ROS accompanying

stress is potentially a physiological by product. Subsequently, in *IL6*-KO mice iron

overloaded by injection of iron dextran, we found that two weeks following BA

administration, cytoplasmic ROS of BM erythroid progenitors is increased (Fig

12B). This upregulated cytoplasmic ROS is accompanied by a concurrent

blunted erythroid differentiation in the BM of the iron overloaded *IL6*-KO mice

(Fig 12C). Given that the DKO is also IL6-deficient but overloaded with iron (due

to lack of *Hamp*), we also looked at cytoplasmic ROS expression in the *Hamp*-

KO and the DKO. We find that two weeks after injection of BA, the *Hamp*-KO and

DKO upregulate cytoplasmic ROS in their BM erythroid progenitors (Fig 12D).

This upregulated ROS was accompanied by an impaired or delayed BM

erythropoiesis, particularly in the DKO (Fig 12E), in line with our hypothesis that

lack of IL6 in combination with iron overload is deleterious to BM erythroid

differentiation. Furthermore, diminished BM erythropoiesis and upregulated ROS

in the DKO and the *Hamp*-KO was also accompanied an upregulation of the

cytokines IFNy and TNFα in both the genotypes (Fig 12F).
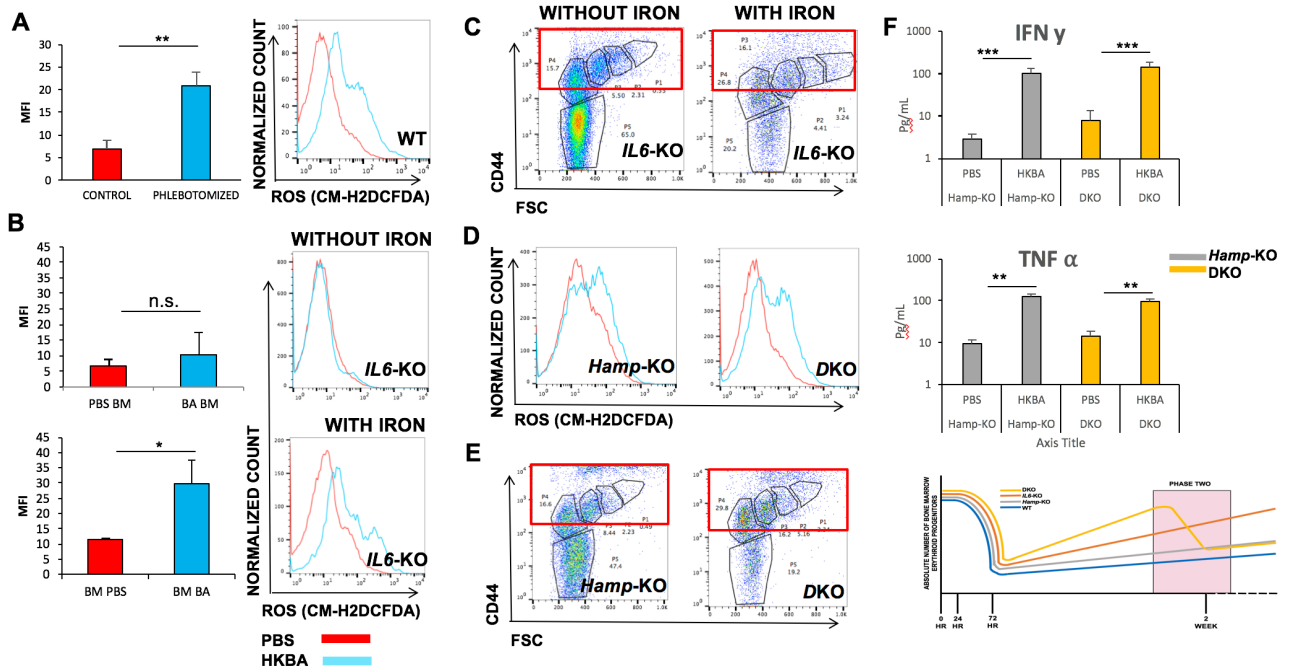
Figure 2.12. ROS upregulation is a physiological by-product of stress erythropoiesis, but becomes detrimental in the presence of iron overload. * P<0.05, ** P<0.01, *** P<0.001 (A) Flow cytometric analysis of cytoplasmic ROS of BM erythroid progenitors in mice phlebotomized to induce acute stress erythropoiesis. Cytoplasmic ROS expression in erythroid progenitors was measured and quantified as described in Figure 10A. n=3, histogram of sample from one representative mouse is shown. (B) Flow cytometric analysis of cytoplasmic ROS of BM erythroid progenitors in PBS and BA injected *IL6*-KO mice without and with the injection of iron dextran to induce iron overload. Cytoplasmic ROS expression in erythroid progenitors was measured and quantified as described in Figure 10A. n=4, histogram of sample from one representative mouse is shown. (C) Flow cytometric analysis of BM terminal erythroid differentiation (selection method described in Figure 3) in BA injected *IL6*-KO mice without and with the injection of iron dextran to induce iron overload. n=4, flow cytometric dot plots of a sample from one representative mouse is shown. Red box indicates erythroid progenitors. (D) Flow cytometric analysis of cytoplasmic ROS of BM erythroid progenitors in PBS and BA injected *Hamp*-KO and DKO mice. Cytoplasmic ROS expression in erythroid progenitors was measured and quantified as described in Figure 10A. n=5, histogram of sample from one representative mouse is shown. (E) Flow cytometric representation of terminal erythroid differentiation (as described in Figure 3), for *Hamp*-KO and

48

DKO mice 2 weeks after BA injection. Red box indicates erythroid progenitors, n=5. (F) IFN y and TNFα cytokine levels in serum of *Hamp*-KO and DKO mice 2 weeks after injection of BA, in comparison to PBS injected controls were plotted in bar graphs. Grey bars indicate *Hamp*-KO and yellow bars indicate DKO, n=5.

Additionally, when we looked at ROS generation in splenic erythroid progenitors of BA injected *IL6*-KO mice with and without the treatment of iron dextran to induce iron overload, we found no difference (Fig 13A). Moreover, the spleen of the *Hamp*-KO and the DKO show no increase in cytoplasmic ROS and remain protected (Fig 13B).
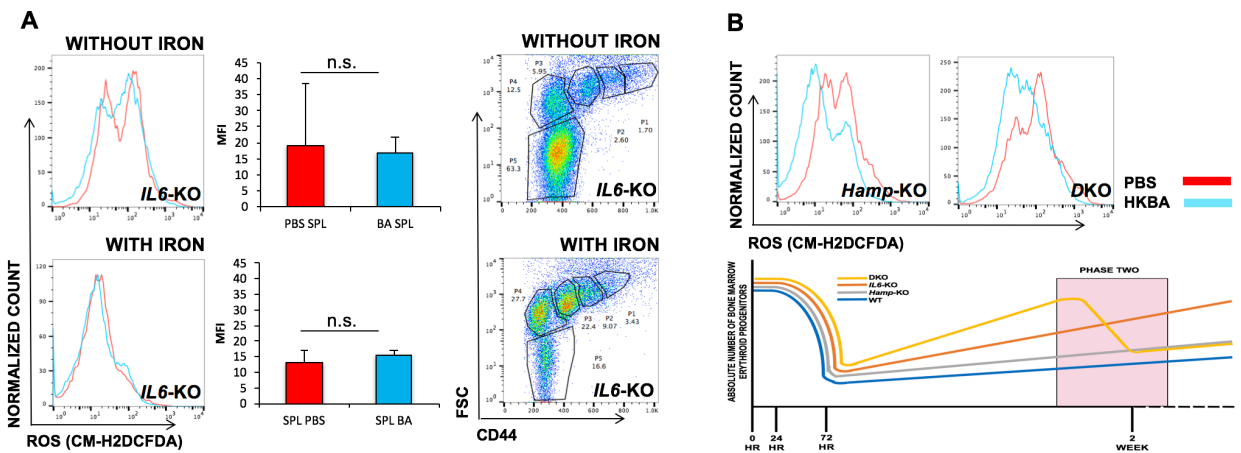
Figure 2.13. The spleen is protected from ROS upregulation under conditions of iron overload. As in Fig 12B; but indicating cytoplasmic ROS in splenic erythroid progenitors of *IL6*-KO mice, without and with the injection of iron dextran to induce iron overload and additionally showing erythroid differentiation in the spleen under the same conditions, n=4. (B) As in Fig 12D, but indicating cytoplasmic ROS levels in splenic erythroid progenitors of *Hamp*-KO and DKO mice, two weeks after injection of BA, n=5.

Finally, to investigate the presence of NTBI in the WT mice, as an explanation of ROS possibly impairing BM erythroid recovery in these animals, we looked at serum iron and transferrin saturation two weeks after administration of BA. We found that although the serum iron showed no difference upon BA injection in the second phase of recovery (Fig 14A), the transferrin saturation decreases (Fig 14B) indicating presence of iron in the serum not bound to transferrin potentially capable of damage in this phase.
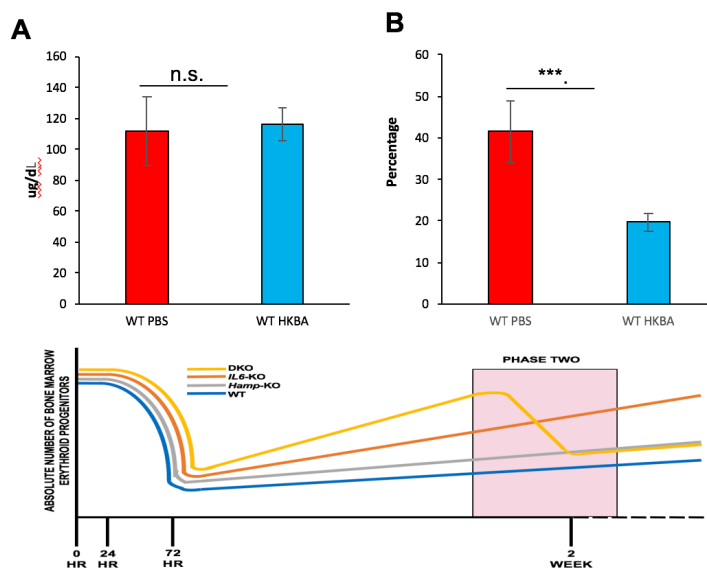
Figure 2.14. During phase two of recovery under inflammation, the WT shows presence of iron in the serum not bound to transferrin. * P<0.05, ** P<0.01, *** P<0.001 (A) Serum iron in PBS and BA injected WT mice two weeks after injection of BA, n=5. (B) Transferrin saturation in PBS and BA injected WT mice two weeks after injection of BA, n=5.

Based on this above data, we were able to generate a model of erythroid recovery under AI, in the context of iron overloading conditions and lack of IL6 (Fig 15). Under stress erythropoiesis, BM erythroid progenitors can upregulate

production of ROS. Under inflammation, this upregulated ROS produced as a result of erythropoietic stress can downregulate erythroid recovery in the BM. This ROS mediated impaired erythroid recovery can be inhibited by lack of IL6 but this protective effect under absence of IL6 is reversed in the presence of either high levels of iron or by a concurrent absence of Hamp.
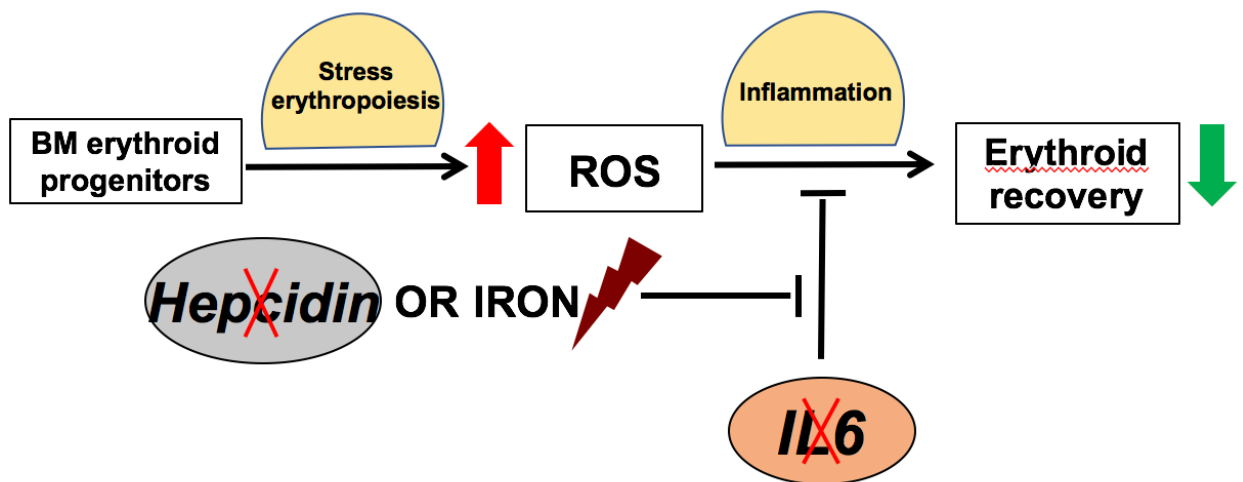
Figure 2.15. A model of erythroid recovery under AI. Under condition of stress erythropoiesis, erythroid progenitors upregulate production of ROS. Under inflammation, this stress mediated upregulation of ROS impairs erythroid recovery. Absence of IL6 inhibits upregulated ROS but this process is reversible under conditions of iron overload, by lack of Hamp or administration of iron.

Chapter Three

Methods

BA induced model of inflammation

Heat killed *Brucella abortus* was acquired from the United States Department of

Agriculture, National Veterinary services laboratories and prepared as described

by Sasu *et al* (204). A single dose of 5 X 10^8 particles of BA was injected IP in

mice, which were sacrificed at the stated time points for harvesting organs,

processing cells, and further analysis. All animals were age and sex matched-

male and five months of age. WT and *IL6*-KO mice were purchased from

Jackson Laboratories, and *Hamp*-KO mice were a gift from the laboratory of Dr.

Thomas Ganz at UCLA. Peripheral blood hemoglobin of all animals was

monitored weekly following injection of BA and animals that did not develop

anemia (Hb > 11g/dL, 7 days after injection of BA) were excluded from analysis.

All animal studies were carried out in accordance with protocols approved by the

Institutional Animal Care and Use Committee, Laboratory Animal Services at the

Children's Hospital of Philadelphia.

Mouse sacrifice and tissue harvest

Mice were anaesthetized using isoflurane and euthanized by cervical dislocation.

A midline incision on the ventral side was used to expose the internal organs

including the spleen, which was harvested. The femur and tibia of one leg were

also harvested and all organs were stored temporarily on ice in a solution of 1% PBS BSA (buffer). The femur and tibia were cut on both ends and a 26G X ½ needle connected to a 5 mL syringe was used to aspirate the bones with 5 mL of buffer to collect BM cells. The spleen was crushed between two glass slides to break down the outer membrane and a similar 26G ½ needle connected to a 5 mL syringe was used to break down cellular aggregates in 5 mL of buffer. Harvested BM and spleen cells were then passed through a 40 micron filter and subsequently used for flow cytometric staining.

Collection of serum and blood for CBC

To prepare serum, 750 uL of blood was withdrawn retro-orbitally with a non-heparinized capillary tube from anesthetized animals immediately prior to euthanasia. The blood was collected and stored at room temperature for 2 hours, and then centrifuged at 3000 rpm for 30 minutes. The supernatant (serum) was collected and stored at -80°C for further analysis

For CBC, 40 uL of blood was withdrawn retro orbitally with a heparinized capillary tube from anesthetized animals and analyzed for CBC by the Advia 120 Hematology system.

Flow cytometric analysis

To evaluate erythropoiesis, 10^{6} cells of the BM and the spleen were aliquoted and washed with 1% PBS BSA (centrifugation at 300 g for 5 minutes). After discarding the supernatant, the cells were stained with TER119 APC, CD71 FITC

and CD44 PE at a dilution of 0.5 uL of the antibody suspended in 100 uL of

staining buffer (1% PBS BSA). After 30 minutes of incubation on ice in the dark,

cells were washed and re-suspended in 200 uL of staining buffer for analysis by

flow cytometry. Cells were sorted using a BD FACS Calibur and results were

analyzed on FloJo software (TreeStar).

To examine mitochondrial superoxide production in erythroid progenitors, cells

were stained with TER119 APC, CD29 FITC as described, and washed with PBS

only. Following wash, cells were incubated with Mitosox Red (Life Technologies,

Thermo Fischer Scientific) at a concentration of 5 μM for 15 minutes at 37°C in

the dark and sorted using a BD FACS Calibur.

For examining ROS in erythroid progenitors, cells were stained with TER119

APC, CD29 FITC as described, and washed with PBS only. Following wash, cells

were incubated with CM-H$_2$DCFDA (Life Technologies, Thermo Fischer

Scientific) at a concentration of 25 nM for 15 minutes at 37°C in the dark and

sorted using a BD FACS Calibur.

RBC Lifespan experiment

0.875 mg of Sulfo-NHS-Biotin (Thermo Fischer Scientific) was dissolved in 200

uL of PBS and injected intravenously in each mouse. 12 hours following injection

of Biotin, peripheral blood collected from the mouse tail was stained with

streptavidin PE, and PE fluorescence was analyzed by flow cytometry as a

measure of biotinylated RBC. 24 hours following injection of Biotin the mice were

injected with BA as described. 4, 7, 11 and 14 days following injection of BA,

peripheral blood collected from the mouse tail was stained with streptavidin PE and PE fluorescence was analyzed by flow cytometry as a measure of biotinylated RBC.

Oxyblot

Whole bone marrow and spleen cells were washed with 1% PBS BSA. Following centrifugation at 300 g for 5 minutes, supernatant was discarded and cell pellets were stored at -80C. Frozen cell pellets were treated with RIPA buffer for extraction of cell lysate proteins. Subsequently they were subjected to derivatization reaction with 2,4, dinitrophenyl hydrazine and oxidized proteins were detected with an anti-dinitrophenyl hydrazine antibody (Oxyblot protein oxidation detection kit-EMD Millipore) as described by Marinkovic *et al*.

Iron Dextran experiment

24 hours prior to injection of BA, mice were injected IP with iron dextran (Sigma Aldrich) at 1 gram/kg body weight of each mouse. 6 days following injection of BA mice were injected with a second dose of iron dextran and sacrificed 14 days following injection of BA. Sacrificed animals were analyzed for erythropoiesis and ROS production as described previously.

Serum Iron and transferrin saturation experiment

Iron parameters in the serum were tested as described by Gardenghi *et al* (273) using a diagnostic iron TIBC (total iron binding content) kit from Pointe Scientific.

Cytokine analysis

Serum cytokines were measured by the Biolegend Legendplex, a bead based sandwich immunoassay, following instructions on the assay kit (Bioelgend).

Statistics

The data is presented as mean $\pm$ SD (standard deviation). An unpaired 2-tailed Student *t* test was used to assess significance (for comparison of two groups of samples with normal distribution by Shapiro Wilk's normality test). Graphpad prism 7 and Microsoft Excel for Mac 2016 software was used. $P < 0.05$ was considered statistically significant.

Chapter 4

Discussion and Future Perspectives

The etiology of anemia in the context of inflammation, particularly one caused by pathogenic infections, is such that providing iron administration to ameliorate anemia in clinical settings is detrimental to disease prognosis and patient recovery. This warrants the need to examine cellular responses and molecular mechanisms underlying AI. Thus, the study of AI requires well established mammalian systems capable of simulating both the anemia and the inflammatory reaction seen in clinical settings. The BA model not only shows hallmarks of an inflammatory reaction, but also simultaneously induces significant anemia (in contrast to LPS or CFA models), and hence is being used as an ideal murine model to study AI.

The first phase of response to BA in terms of cytokine upregulation, change in iron parameters, and impaired BM erythropoiesis in WT animals has been characterized in literature by others as well as by us. However, in this study, we were able to identify and characterize a second phase of response to BA. Like the first phase, the second phase is marked by an upregulation of cytokines. However, unlike the first phase, the second phase highlights a protective effect of lack of IL6 and a concurrent detrimental effect of iron overload. This divergence of BM erythroid recovery in the second phase

57

prompted us to investigate cellular responses impeding BM erythropoiesis. We found that upregulated ROS in BM erythroid progenitors positively correlates with impaired BM erythropoiesis and that this can be aggravated by iron overload. Moreover, in our studies we found that while absence of IL6 is protective, high levels of iron can impair BM erythropoiesis in the same animals. Our study not only elucidates altered mitochondrial ROS production in response to BA, but also highlights a ROS mediated deleterious effect on BM erythropoiesis by conditions of iron overload under AI.

We noticed an upregulation of ROS under stress erythropoiesis in WT mice. We also showed that upregulation of ROS is a by-product of stress erythropoiesis induced by phlebotomy. However, as WT animals do not show the same improvement in BM erythropoiesis as *IL6*-KO mice, we postulated that increased ROS levels mediated by stress erythropoiesis + inflammation limits or slows down erythroid recovery. Iron not bound to transferrin has been previously linked to oxidative stress. Additionally, the potential presence of NTBI/LPI in WT animals, during the second phase, could also affect negatively erythropoiesis in presence of inflammation. To test the role of NTBI, we are currently studying the presence of a labile iron pool in mice with impaired erythroid recovery under AI.

Moreover, it will also be worthwhile to investigate the presence of acute phase-reactant proteins such as Ferritin in the serum that are capable of binding to NTBI and potentially contributing to oxidative damage. Furthermore, it is possible that certain iron transporters such as Zip8, that import NTBI into erythroid progenitors in the BM might be upregulated under AI, allowing

58

excessive non-transferrin linked iron to impair differentiation of erythroid progenitors in the BM. In line with this theory, we would also like to test whether metal ion transporters such as Zip8 or Zip14 are upregulated in erythroid cells of mice that exhibit impaired erythroid recovery.

Although NTBI can potentially impede BM erythropoiesis in the WT mice under AI, our results with the *IL6*-KO mice suggest that there might be an NTBI independent negative influence of the presence of this cytokine in BM erythropoiesis under AI. There are multiple studies showing increased NFκB promoter activation and IL6 production linked to upregulated ROS in murine skeletal muscle cells but whether this relationship extends to other cell types remains to be seen (209, 210, 211, 212). However, this evidence combined with our results that ROS is not upregulated in the absence of IL6 strengthens the idea that the link between IL6 and BM erythropoiesis might lie within ROS itself. How the mitochondrial generation of ROS impinges on the STAT3 dependent pathway downstream of the IL6 receptor or vice versa, still remains unknown.

Our work shows a positive correlation between upregulation of ROS and a decline of BM erythroid differentiation. Given that we did not detect an activation of apoptosis in our ROS upregulated cells (not shown), our negative data point to the possible role of non-apoptotic forms of programmed cell death downstream of ROS upregulation, such as necroptosis. This idea is supported by the upregulation of the cytokine TNFα in both of our phases of response to BA, as this cytokine has been implicated as a key mediator of necroptosis, and derives its name from the process (142, 143, 144, 145, 146). Furthermore, in the past

decade there has been substantial work linking TNFα to ROS upregulation,

although the evidence supporting the role of NFκB in this crosstalk between the

two remains contradictory (135). Given the obvious role of TNFα in necroptosis

and some literature suggesting it's connection to ROS, we can speculate that

upregulation of TNFα in combination with inflammation, ROS and excess of NTBI

could trigger necroptosis and inhibit terminal erythroid differentiation in the BM.

To test a potential role of necroptosis in AI, we are currently investigating

recovery from BA in RIP3K KO mice that are resistant to necroptosis. Moreover,

to further elucidate lineage specific impact of the absence of IL6 in protecting BM

erythropoiesis under AI, we are crossing IL6 receptor (gp80) floxed mice with

Epo R Cre and Vav Cre animals.

From a clinical point of view, current treatments for AI include

erythropoiesis stimulating agents in combination with oral or intravenous iron

administration. IL6 blocking antibodies such as Tocilizumab have also been

used. However, iron supplementation in the context of AI under active infections

can potentially prevent pathogen clearance and disease prognosis. While

blocking IL6 is effective, use of this also precludes any supportive functions of

this cytokine in resolving inflammation. There is a need to parse out the

independent contributions of this cytokine in anemia and in inflammation, to

target specific IL6 mediated cellular responses for treatment of anemia without

affecting its function as a primary responder under inflammation. Our results

provide clues to intracellular responses that can be targeted for these purposes.

To summarize, our study identifies the presence of a second phase of response to BA, and characterizes this phase in terms of recovery in the absence of IL6 and in the presence of iron overloading conditions. Additionally, our study also detects ROS as a cellular response accompanying impaired erythroid recovery and suggests the potential of iron not bound to transferrin in damaging BM erythropoiesis.

AI is a hallmark of numerous chronic inflammatory conditions and affects a large number of individuals. Production of inflammatory cytokines and anemia are also particularly acute in conditions such as sepsis, and this combination is often lethal. Therefore, there is a need to investigate underlying pathways contributing to the resulting anemia. Our study could potentially provide evidence of cellular responses that can be targeted in conditions of dysregulated iron metabolism for therapeutic benefits.

Chapter Five

References

1. Lewis GK. and Drickamer HG. High pressure Mossbauer resonance studies of the conversion of Fe(III) to Fe(II) in Ferric halides. PNAS. 1968 Oct;61(2):414-21.

2. Rice-Evans C and Baysal E. Iron-mediated oxidative stress in erythrocytes. Biochem J. 1987 May 15;244(1):191-6.

3. Agarwal N. and Prchal JT. Anemia of chronic disease (Anemia of inflammation). Acta Hematol. 2009;122(2-3):103-8

4. Cartwright GE, Lauritsen MA, Jonae PJ, Merrill IM and Wintrobe MM. The anemia of infection. I. Hypoferremia, Hypercupremia, and alterations in porphyrin metabolism in patients. J Clin Invest. 1946 Jan;25(1):65-80

5. Ariel I, Rekers PE, Pack GT and Rhoads CP. Metabolic studies in patients with cancer of the gastro-intestinal tract: X-hypoproteinemia and anemia in patiens with gastric cancer. Ann Surg. 1943 Sep;118(3):366-71.

6. Alexander WR, Richmond J, Roy LM and Duthie JJ. Nature of anemia in rheumatoid arthritis. II. Survival of transfused erythrocytes in patients with rheumatoid arthritis. Ann Rheum Dis. 1956 Mar;15(1):12-20.

7. Donahue RE, Johnson MM, Zon LI, Clark SC and Groopman JE Suppression of in vitro hematopoiesis following human immunodeficiency virus infection. Nature. 1987 Mar 12-18;326(6109):200-3

8. Pol S, Driss F, Devergie A, Brechot C, Berthelot P and Gluckman E. Is hepatitis C virus involved in hepatitis associated aplastic anemia? Ann Intern Med. 1990 Sep 15;113(6):435-7.

9. DE Kretser AJ and Goldfarb S. Hemolytic anemia in a tuberculosis patient with liver disease receiving stilboestrol. Tubercle. 1958 Oct;39(5):302-6.

10. Sheehy TW and Cannon NJ. Hemaotologic complications of inflammatory bowel disease. J Med Assoc State Ala. 1974 Sep;44(3):121-8, 134

11. Pisciotta AV, Giliberti JJ, Greenwart TJ and Engstrom WW. Acute hemolytic anemia in disseminated lupus erythematosus; treatment with cortisone; report of case. Am J Clin Pathol. 1951 Dec;21(12):1139-44

12. Loge JP, Lange RD and Moore CV. Characterization of the anemia of chronic renal insufficiency. J Clin Invest. 1950 Jun;29(6):830-1

13. Durham JR. Cardiac dysfunction with severe anemia. Del Med J. 1947 Jul;19(7):132-4.

14. Hutton MM, Prentice CR, Allison ME, Duguid WP, Kennedy AC, Struthers NW and McNicol GP. Renal homotransplant rejection associated with microangiopathic hemolytic anemia. Br Med J. 1970 Jul 11;3(5714):87-8.

15. Maynor L and Brophy DF. Risk of infection with intravenous iron therapy. Ann Pharmacother. 2007 Sep;41(9):1476-80.

16. Gregory CJ and Eaves AC. Three stages of erythropoietic progenitor cell differentiation distinguished by a number of physical and biological properties. Blood. 1978 Mar;51(3):527-37

17. Liu J Zhang J, Ginzburg Y, Li H, Xue F, De Franceschi L, Chasis JA, Mohandas N and An X. Qualitative analysis of murine terminal erythroid differentiation in vivo: novel method to study normal and disordered erythropoiesis. Blood. 2013 Feb 21;121(**8**): e43-9.

18. Hu J, Liu J, Xue F, Halverson G, Reid M, Guo A, Chen L, Raza A, Galili N, Jaffray J, Lane J, Chasis JA, Taylor N, Mohandas N and An X. Isolation and functional characterization of human erythroblasts at distinct stages: Implications for understanding of normal and disordered erythropoiesis in vivo. Blood. 2013 Apr 18;121(16):3246-53.

19. Laurell CB. What is the function of transferrin in plasma? Blood. 1951 Feb;6(2):183-7.

20. Fletcher J and Huehns ER. Significance of the binding of iron by transferrin. Nature. 1967 Aug 5;215(5101):584-6.

21. Vogel W, Bomford A, Young S and Williams R. Heterogenous distribution of transferrin receptor on parenchymal and non-parenchymal liver cells: biochemical and morphological evidence. Blood. 1987 Jan;69(1):264-70.

22. Galbraith GM, Galbraith RM, Temple A and Faulk WP. Demonstration of transferrin receptors on human placental trophoblasts. Blood. 1980 Feb;55(2):240-2.

23. Rana KS, Varma N and Dash S. Iron overload: Detection using a micromethod for iron binding capacity. Med Lab. Sci. 1991 Jan;48(1):27-30.

24. Ahmed NK, Hanna M and Wang W. Non transferrin bound serum iron in thalassemia and sickle cell patients. Int J Biochem. 1986;18(10):953-6.

25. Livrea MA, Tesoriere L, Pintaudi AM, Calabrese A, Maggio M, Freisleben HJ, D'Arpa D, D'Anna R, Bongiorno A. Oxidative stress and anti oxidant status in beta-thalassemia major: iron overload and depletion of lipid soluble anti oxidants. Blood. 1996 Nov 1;88(9):3608-14.

26. Cabantchik Z, Breuer W, Zanninelli G and Cianciulli P. LPI-labile plasma iron in iron overload. Best Pract Red Clin Haematol. 2005 Jun;18(2):277-87.

27. Kakhlon O and Cabantchik Z. The labile iron pool: characterization, measurement and participation in cellular processes. Free Radic Biol Med. 2002 Oct 15;33(8):1037-46.

28. Kruszewski M. Labile iron pool: the main determinant of cellular response to oxidative stress. Mutat Res. 2003 Oct 29;531(1-2):81-92.

29. Wang CY, Jenkitkasemwong M, Duarte S, Sparkman BK, Shawki A, Mackenzie B and Knutson MD. ZIP8 is an iron and zinc transporter whose cell surface expression is upregulated by cellular iron loading. J Biol Chem. 2012 Oct 5;287(41):34032-43.

30. Kristiansen M, Graversen JH, Jacobsen C, Sonne O, Hoffman HJ, Law SK and Moestrup SK. Identification of the hemoglobin scavenger receptor. Nature. 2001 Jan 11;409(6817):198-201.

31. Fleming RE, Migas MC, Zhous X, Jiang J, Britton RS, Brunt EM, Tomatsu S, Waheed A, Bacon BR and Sly WS. Mechanism of increased iron absorption in murine model of hereditary hemochromatosis: increased duodenal expression of the iron transporter DMT1. Proc Natl Acad Sci U S A. 1999 Mar 16;96(6):3143-8.

32. McKie AT, Barrow D, Latunde-Dada GO, Rolfs A, Sager G, Mudaly E, Mudaly M, Richardson C, Barlow D, Bomford A, Peters TJ, Raja KB, Shirali S, Hediger MA, Farzaneh F and Simpson RJ. An iron regulated ferric reductase associated with the absorption of dietary iron. Science. 2001 Mar 2;291(5509):1755-9.

33. Kay MM. Mechanism of removal of senescent cells by human macrophages in situ. Proc Natl Acad Sci U S A. 1975 Sep;72(9):3521-5.

34. Tsukamoto H, Lin M, Ohata M, Giulivi C, French SW and Brittenham G. Iron primes hepatic macrophages for NF kappa B activation in alcoholic liver injury. Am J Physiol. 1999 Dec;277(6 Pt 1): G1240-50.

35. Donovan A, Brownlie A, Zhou Y, Shepard J, Pratt SJ, Moynihan J, Paw BH, Drejer A, Barut B, Zapata A, Law TC, Brugnara C, Lux SE, Pinkus GS, Pinkus JL, Kingsley PD, Palis J, Fleming MD, Andrews NC and Zon LI. Positional cloning of zebrafish ferroportin 1 identifies a convsered vertebrate iron exporter. Nature. 2000 Feb 17;403(6771):776-81.

36. Abboud S and Haile DJ. A novel mammalian iron regulated protein involved in intracellular iron metabolism. J Biol Chem. 2000 Jun 30;275(26):19906-12.

37. Levine WG and Peisach J. Mechanism of iron stimulation of the enzymatic activitiy of ceruloplasmin. Nature. 1965 Jul 24;207(995):406-7.

38. Vulpe CD, Kuo YM, Murphy TL, Cowley L, Askwith C, Libina N, Gitschier J and Anderson GJ. Hepaestin, a ceruloplasmin homolog implicated in intestinal iron transport, is defective in the sla mouse. Nat Genet. 1999 Feb;21(2):195-9.

39. Park CH, Valore EV, Waring AJ and Ganz T. Hepcidin, a urinary antimicrobial peptide synthesized in the liver. J Biol Chem. 2001 Mar 16;276(11):7806-10.

40. Fleming RE and Sly WS. Hepcidin: a putative iron regulatory hormone relevant to hereditary hemochromatosis and the anemia of chronic disease. Proc Natl Acad Sci U S A. 2001 Jul 17;98(15):8160-2.

41. Rivera S, Nemeth E, Gabayan V, Lopez MA, Farshidi D and Ganz T. Synthetic Hepcidin causes rapid dose dependent hypoferremia and is concentrated in ferroportin containing organs.

42. Fleming RE and Sly WS. Mechanisms of iron accumulation in hereditary hemochromatosis. Annu Rev Physiol. 2002; 64:663-80.

43. De Domenico I, Ward DM, Langelier C, Vaughn MB, Nemeth E, Sundquist WI, Ganz T, Musci G and Kaplan J. The molecular mechanism of Hepcidin-mediated ferroportin down-regulation. Mol Biol Cell. 2007 Jul;18(7):2569-78.

44. Nemeth E, Tuttle MS, Powelson J, Vaughn MB, Donovan A, Ward DM, Ganz T and Kaplan J. Hepcidin regulates cellular iron efflux by binding to ferroportin and inducing its internalization. Science. 2004 Dec 17;306(5704):2090-3.

45. Nicolas G, Chauvet C, Viatte L, Danan JL, Bigard X, Devaux I, Beaumont C, Kahn A and Vaulont S. The gene encoding the iron regulatory peptide

hepcidin is regulated by anemia hypoxia and inflammation. J Clin Invest. 2002 Oct;110(7):1037-44

46. Frazer DM, Wilkins SJ, Becker EM, Vulpe CD, McKie AT, Trinder D, Anderson GJ. Hepcidin expression inversely correlates with the expression of duodenal iron transporters and iron absoroption in rats. Gastroenterology. 2002 Sep;123(3):835-44.

47. Nicolas G, Viatte L, Lou DQ, Bennoun M, Beaumont C, Kahn A, Andrews NC and Vaulont S. Constitutive iron expression prevents iron overload in a mouse model of hemochromatosis. Nat Genet. 2003 May;34(1):97-101.

48. Adamsky K, Weizer O, Amariglio N, Breda L, Harmelin A, Rivella S, Rachmilewitz E and Rechavi G. Decreased hepcidin mRNA expression in thallassemic mice. Br J Haematol. 2004 Jan;124(1):123-4.

49. Papanikolaou G, Samuels ME, Ludwig EH, MacDonald ML, Franchini PL, Dubé MP, Andres L, MacFarlane J, Sakellaropoulos N, Politou M, Nemeth E, Thompson J, Risler JK, Zaborowska C, Babakaiff R, Radomski CC, Pape TD, Davidas O, Christakis J, Brissot P, Lockitch G, Ganz T, Hayden MR and Goldberg YP. Mutations in HFE2 cause iron overload in chromosome 1q-linked juvenile hemochoromatosis. Nat Genet. 2004 Jan;36(1):77-82.

50. Feder JN, Penny DM, Irrinki A, Lee VK, Lebrón JA, Watson N, Tsuchihashi Z, Sigal E, Bjorkman PJ and Schatzman RC. The hemochromatosis gene product complexes with the transferrin receptor and lowers its affinity for ligand binding. Proc Natl Acad Sci U S A. 1998 Feb 17;95(4):1472-7.

51. West AP Jr, Bennett MJ, Sellers VM, Andrews NC, Enns CA and Bjorkman PJ. Comparison of the interactions of transferrin receptor and transferrin receptor 2 with transferrin and the hereditary hemochromatosis protein HFE. J Biol Chem. 2000 Dec 8;275(49):38135-8.

52. Goswami T and Andrews NC. hereditary hemochromatosis protein HFE interaction with transferrin receptor 2 suggests a molecular mechanism for mammalian iron sensing. J Biol Chem. 2006 Sep 29;281(39):28494-8.

53. Andriopoulos B. Junior, Corradini E, Xia Y, Faasse SA, Chen S, Grgurevic L, Knutson MD, Piterangelo A, Vukisevic S, Linn HY and Babitt JL. BMP6 is a key endogenous regulator of hepcidin expression and iron metabolism. Nat Genet. 2009 Apr;41(4):482-7.

54. Meynard D, Kautz L, Darnaud V, Canonne-Hergaux F, Coppin H and Roth MP. Lack of bone morphogenic protein BMP6 induces mass iron overload. Nat Genet. 2009 Apr;41(4):478-81.

55. Zhang AS, Gao J, Koeberl DD and Enns CA. The role of hepatocyte hemojuvelin in the regulation of bone morphogenic protein-6 and hepcidin expression in vivo. J Biol Chem. 2010 May 28;285(22):16416-23.

56. Nili M, Shinde U and Rotwein P. Soluble repulsive guidance molecule c/hemojuvelin is a broad spectrum bone morphogenetic protein (BMP) antagonist and inhibits both BMP2- and BMP6-mediated signaling and gene expression. J Biol Chem. 2010 Aug 6;285(32):24783-92.

57. Silvestri L, Pagani A, Nai A, De Domenico I, Kaplan J and Camaschella C. The serine protease matriptase-2 (TMPRSS6) inhibits hepcidin activation by cleaving membrane hemojuvelin. Cell Metab. 2008 Dec;8(6):502-11.

58. Du X, She E, Gelbart T, Truksa J, Lee P, Xia Y, Khovananth K, Mudd S, Mann N, Moresco EM, Beutler E, Beutler B. The serine protease TMPRSS6 is required to sense iron deficiency. Science. 2008 May 23;320(5879):1088-92.

59. Leung PS, Srai SK, Mascarenhas M, Churchill LJ and Debnam ES. Increased duodenal iron uptake and transfer in a rat model of chronic hypoxia is accompanied by reduced hepcidin expression. Gut. 2005 Oct;54(10):1391-5.

60. Liu Q, Davidoff O, Niss K and Haase VH. Hypoxia-inducible factor regulates hepcidin via erythropoietin-induced erythropoiesis. J Clin Invest. 2012 Dec;122(12):4635-44.

61. Kautz L, Jung G, Valore EV, Rivella S, Nemeth E and Ganz T. Identification of erythroferrone as an erythroid regulator of iron metabolism. Kautz L, Jung G, Valore EV, Rivella S, Nemeth E and Ganz T.

62. Kautz L, Jung G, Du X, Gabayan V, Chapman J, Nasoff M, Nemeth E and Ganz T. Erythroferrone contributes to hepcidin suppression and iron overload in a mouse model of β-thalassemia. Blood. 2015 Oct 22;126(17):2031-7.

63. Volke M, Gale DP, Maegdefrau U, Schley G, Klanke B, Bosserhoff AK, Maxwell PH, Eckardt KU and Warnecke C. Evidence for a lack of a direct transcriptional suppression of the iron regulatory peptide hepcidin by hypoxia-inducible factors. PLoS One. 2009 Nov 18;4(11): e7875.

64. Jongen-Lavrencic M, Peeters HR, Rozemuller H, Rombouts WJ, Martens AC, Vreugdenhil G, Pillay M, Cox PH, Bijser M, Brutel G, Breedveld FC and Swaak AJ. L-6-induced anaemia in rats: possible pathogenetic implications for anemia observed in chronic inflammations. Clin Exp Immunol. 1996 Feb;103(2):328-34.

65. Vecchi C, Montosi G, Zhang K, Lamberti I, Duncan SA, Kaufman RJ, Pietrangelo A. ER_stress_controls iron metabolism through induction of hepcidin. Science. 2009 Aug 14;325(5942):877-80.

66. Medzhitov R. Origin_and_physiological_roles_of_inflammation. Nature. 2008 Jul 24;454(7203):428-35.

67. Ozinsky A, Underhill DM, Fontenot JD, Hajjar AM, Smith KD, Wilson CB, Schroeder L and Aderem A. The repertoire for_pattern_recognition of pathogens by the innate immune system is defined by cooperation between toll-like receptors. Proc Natl Acad Sci U S A. 2000 Dec 5;97(25):13766-71.

68. Ganz T, Selsted ME, Szklarek D, Harwig SS, Daher K, Bainton DF and Lehrer RI. Defensins. Natural peptide antibiotics of human neutrophils. J Clin Invest. 1985 Oct;76(4):1427-35.

69. Qureshi ST, Larivière L, Leveque G, Clermont S, Moore KJ, Gros P and Malo D. Endotoxin-tolerant mice have mutations in_Toll-like_receptor 4 (Tlr4). J Exp Med. 1999 Feb 15;189(4):615-25.

70. Kopp EB, Medzhitov R. The_Toll-receptor family and control of innate immunity. Curr Opin Immunol. 1999 Feb;11(1):13-8.

71. Kouba M, Vanetti M, Wang X, Schäfer M and Höllt V. Cloning of a novel putative G-protein-coupled receptor (NLR) which is expressed in neuronal and lymphatic tissue. FEBS Lett. 1993 Apr 26;321(2-3):173-8.

72. Murillo LS, Morré SA and Peña AS. Toll-like_receptors_and_NOD/CARD_proteins: pattern recognition_receptors_are key elements in the regulation of immune response. Drugs Today (Barc). 2003 Jun;39(6):415-38.

73. Baeuerle PA and Baltimore D. I kappa B: a specific inhibitor of the_NF-kappa B_transcription factor. Science. 1988 Oct 28;242(4878):540-6.

74. Lenardo MJ and Baltimore D. NF-kappa B: a pleiotropic mediator of inducible and tissue-specific gene control. Cell. 1989 Jul 28;58(2):227-9.

75. Kuijpers TW and Roos D. Leukocyte_extravasation: mechanisms and consequences. Behring Inst Mitt. 1993 Aug;(92):107-37.

76. Tessier PA, Naccache PH, Clark-Lewis I, Gladue RP, Neote KS and McColl SR. Chemokine networks in vivo: involvement of C-X-C and C-C_chemokines_in neutrophil_extravasation_in vivo in response to TNF-alpha. J Immunol. 1997 Oct 1;159(7):3595-602.

77. Serhan, CN and Savill, J. Resolution of inflammation: the beginning programs the end. Nature Immunol. 6, 1191–1197 (2005).

78. Bowcock AM, Ray A, Erlich HA and Sehgal PB. The molecular genetics of beta-2 interferon/interleukin-6 (IFN beta 2/IL6) alpha. Ann N Y Acad Sci. 1989; 557:345-52.

79. Durie BG, Vela EE and Frutiger Y. Macrophages as an important source of paracrine IL6 in myeloma bone marrow. Curr Top Microbiol Immunol. 1990; 166:33-6.

80. Akira S. IL-6-regulated transcription factors. Int J Biochem Cell Biol. 1997 Dec;29(12):1401-18.

81. Houssiau F and Van Snick J. IL6 and the T-cell response. Res Immunol. 1992 Sep;143(7):740-3.

82. Van Dam M, Müllberg J, Schooltink H, Stoyan T, Brakenhoff JP, Graeve L, Heinrich PC and Rose-John S. Structure-function analysis of interleukin-6 utilizing human/murine chimeric molecules. Involvement of two separate domains in receptor binding. Biol Chem. 1993 Jul 15;268(20):15285-90.

83. Dodds RA, Merry K, Littlewood A and Gowen M. Expression of mRNA for IL1 beta, IL6 and TGF beta 1 in developing human bone and cartilage. J Histochem Cytochem. 1994 Jun;42(6):733-44.

84. Ogawa M. IL6 and haematopoietic stem cells. Res Immunol. 1992 Sep;143(7):749-51.

85. Krönke M, Schütze S, Scheurich P, Meichle A, Hensel G, Thoma B, Kruppa G and Pfizenmaier K. Tumour necrosis factor signal transduction. Cell Signal. 1990;2(1):1-8.

86. Kull FC Jr. The TNF receptor in TNF-mediated cytotoxicity. Nat Immun Cell Growth Regul. 1988;7(5-6):254-65.

87. Strieter RM, Kunkel SL, Showell HJ, Remick DG, Phan SH, Ward PA and Marks RM. Endothelial cell gene expression of a neutrophil chemotactic factor by TNF-alpha, LPS, and IL-1 beta. Science. 1989 Mar 17;243(4897):1467-9.

88. Feingold KR and Grunfeld C. Tumor necrosis factor-alpha stimulates hepatic lipogenesis in the rat in vivo. J Clin Invest. 1987 Jul;80(1):184-90.

89. Srinivasula SM, Ahmad M, Lin JH, Poyet JL, Fernandes-Alnemri T, Tsichlis PN and Alnemri ES. CLAP, a novel caspase recruitment domain-containing protein in the tumor necrosis factor receptor pathway, regulates NF-kappaB activation and apoptosis. J Biol Chem. 1999 Jun 18;274(25):17946-54.

90. Rrinki KM, Mallilankaraman K, Thapa RJ, Chandramoorthy HC, Smith FJ, Jog NR, Gandhirajan RK, Kelsen SG, Houser SR, May MJ, Balachandran S and Madesh M. Requirement of FADD, NEMO, and BAX/BAK for aberrant mitochondrial function in tumor necrosis factor alpha-induced necrosis. Mol Cell Biol. 2011 Sep;31(18):3745-58.

91. Grunfeld C and Palladino MA Jr. Tumor necrosis factor: immunologic, antitumor, metabolic, and cardiovascular activities. Adv Intern Med. 1990; 35:45-71.

92. Gifford GE and Lohmann-Matthes ML. Gamma interferon priming of mouse and human macrophages for induction of tumor necrosis factor production by bacterial lipopolysaccharide. J Natl Cancer Inst. 1987 Jan;78(1):121-4.

93. T I Roach, C H Barton, D Chatterjee, F Y Liew and J M Blackwell Opposing effects of interferon-gamma on iNOS and interleukin-10 expression in lipopolysaccharide- and mycobacterial lipoarabinomannan-stimulated macrophages. Immunology. 1995 May; 85(1): 106–113.

94. Argyrios N Theofilopoulos, Stefanos Koundouris, Dwight H Kono and Brian R Lawson. The role of IFN-gamma in systemic lupus erythematosus: a challenge to the Th1/Th2 paradigm in autoimmunity. Arthritis Res. 2001; 3(3): 136–141.

95. R Ito, M Shin-Ya, T Kishida, A Urano, R Takada, J Sakagami, J Imanishi, M Kita, Y Ueda, Y Iwakura, K Kataoka and T Okanoue, O Mazda. Interferon-gamma is causatively involved in experimental inflammatory bowel disease in mice. Clin Exp Immunol. 2006 Nov; 146(2): 330–338.

96. Dromparis P and Michelakis ED. Mitochondria in vascular health and disease. Annual Rev. Physiol. 2013; 75:95-126.

97. Sherratt HS. Mitochondria: structure and function. Rev Neurol(Paris). 1991;147(6-7):417-30.

98. Slater EC. Mechanism of phosphorylation in the respiratory chain. Nature. 1953 Nov 28;172(4387):975-8.

99. Green DE, Ziegler DM and Doeg KA. Sequence of components in the succinic chain of the mitochondrial electron transport system. Arch Biochem Biophys. 1959 Nov; 85:280-2.

100. Giannoni G. The organization of the respiratory chain in mitochondria. Minerva Med. 1962 Jul 4; 53:2063-6.

101. King TE and Takemori S. Reconstitution of respiratory-chain systems. VIII. Reconstitution of a succinate-cytochrome c reductase system. Biochim Biophys Acta. 1962 Oct 8;64: 194-6.

102. Grinius LL, Guds TI and Skulachev VP. Arrangement of the electric potential-generating redox chain in the mitochondrial membrane. J Bioenerg. 1971 May;2(2):101-13.

103. Chance B. Fluorescent probe environment and the structural and charge changes in energy coupling of mitochondrial membranes. Proc Natl Acad Sci U S A. 1970 Oct;67(2):560-71.

104. Liu S, Jiao X, Wang X and Zhang L. Interaction of electron leak and proton leak in respiratory chain of mitochondria--proton leak induced by superoxide from an electron leak pathway of univalent reduction of oxygen. Sci China C Life Sci. 1996 Apr;39(2):168-78.

105. Paradies G, Petrosillo G, Pistolese M and Ruggiero FM. The effect of reactive oxygen species generated from the mitochondrial electron transport chain on the cytochrome c oxidase activity and on the cardiolipin content in bovine heart submitochondrial particles. FEBS Lett. 2000 Jan 28;466(2-3):323-6.

106. Ide T, Tsutsui H, Kinugawa S, Utsumi H, Kang D, Hattori N, Uchida K, Arimura Ki, Egashira K and Takeshita A. Mitochondrial electron transport complex I is a potential source of oxygen free radicals in the failing myocardium. Circ Res. 1999 Aug 20;85(4):357-63.

107. Liu Y, Fiskum G and Schubert D. Generation of reactive oxygen species by the mitochondrial electron transport chain. J Neurochem. 2002 Mar;80(5):780-7.

108. McLennan HR and Degli Esposti M. The contribution of mitochondrial respiratory complexes to the production of reactive oxygen species. J Bioenerg Biomembr. 2000 Apr;32(2):153-62.

109. Prough RA and Masters BS. Studies on the NADPH oxidase reaction of NADPH-cytochrome C reductase. I. The role of superoxide anion. Ann N Y Acad Sci. 1973; 212:89-93.

110.   Nishikimi M. The generation of superoxide anion in the reaction of tetrahydropteridines with molecular oxygen. Arch Biochem Biophys. 1975 Jan;166(1):273-9.

111.   Keele BB Jr, McCord JM and Fridovich I. Superoxide dismutase from escherichia coli B. A new manganese-containing enzyme. J Biol Chem. 1970 Nov 25;245(22):6176-81.

112.   Zimmermann R, Flohé L, Weser U and Hartmann HJ. Inhibition of lipid peroxidation in isolated inner membrane of rat liver mitochondria by superoxide dismutase. FEBS Lett. 1973 Jan 15;29(2):117-20.

113.   Wardman P and Candeias LP. Fenton chemistry: an introduction. Radiat Res. 1996 May;145(5):523-31.

114.   Nohl H, Jordan W and Hegner D. Mitochondrial formation of OH Radicals by an ubisemiquinone-dependent reaction an alternative pathway to the iron-catalysed Haber-Weiss cycle. Hoppe Seylers Z Physiol Chem. 1982 Jun;363(6):599-607.

115.   Fischbacher A, von Sonntag C and Schmidt TC. Hydroxyl radical yields in the Fenton process under various pH, ligand concentrations and hydrogen peroxide/Fe(II) ratios. Chemosphere. 2017 May 7; 182:738-744.

116.   Bors W, Michel C and Saran M. On the nature of biochemically generated hydroxyl radicals. Studies using the bleaching of p-nitrosodimethylaniline as a direct assay method. Eur J Biochem. 1979 Apr;95(3):621-7.

117.   Pani G, Colavitti R, Bedogni B, Fusco S, Ferraro D, Borrello S and Galeotti T. Mitochondrial superoxide dismutase: a promising target for new anticancer therapies. Curr Med Chem. 2004 May;11(10):1299-308.

118.   Ott M, Gogvadze V, Orrenius S and Zhivotovsky B. Mitochondria, oxidative stress and cell death. Apoptosis. 2007 May;12(5):913-22.

119.   Halestrap AP, McStay GP and Clarke SJ. The permeability transition pore complex: another view. Biochimie. 2002 Feb-Mar;84(2-3):153-66.

120.   Jacobson J and Duchen MR. Mitochondrial oxidative stress and cell death in astrocytes--requirement for stored Ca2+ and sustained opening of the permeability transition pore. J Cell Sci. 2002 Mar 15;115(Pt 6):1175-88.

121.	Leung AW and Halestrap AP. Recent progress in elucidating the molecular mechanism of the mitochondrial permeability transition pore. Biochim Biophys Acta. 2008 Jul-Aug;1777(7-8):946-52.

122.	Liu X, Kim CN, Yang J, Jemmerson R and Wang X. Induction of apoptotic program in cell-free extracts: requirement for dATP and cytochrome c. Cell. 1996 Jul 12;86(1):147-57.

123.	Kluck RM, Bossy-Wetzel E, Green DR and Newmeyer DD. The release of cytochrome c from mitochondria: a primary site for Bcl-2 regulation of apoptosis. Science. 1997 Feb 21;275(5303):1132-6.

124.	Scarlett JL and Murphy MP. Release of apoptogenic proteins from the mitochondrial intermembrane space during the mitochondrial permeability transition. FEBS Lett. 1997 Dec 1;418(3):282-6.

125.	Itoh K, Tong KI and Yamamoto M. Molecular mechanism activating Nrf2-Keap1 pathway in regulation of adaptive response to electrophiles. Free Radic Biol Med. 2004 May 15;36(10):1208-13.

126.	Mann GE, Niehueser-Saran J, Watson A, Gao L, Ishii T, de Winter P and Siow RC. Nrf2/ARE regulated antioxidant gene expression in endothelial and smooth muscle cells in oxidative stress: implications for atherosclerosis and preeclampsia. Sheng Li Xue Bao. 2007 Apr 25;59(2):117-27.

127.	Yoon S, Woo SU, Kang JH, Kim K, Kwon MH, Park S, Shin HJ, Gwak HS and Chwae YJ. STAT3 transcriptional factor activated by reactive oxygen species induces IL6 in starvation-induced autophagy of cancer cells. Autophagy. 2010 Nov;6(8):1125-38.

128.	Zhang Y, Liu L, Jin L, Yi X, Dang E, Yang Y, Li C and Gao T. Oxidative stress-induced calreticulin expression and translocation: new insights into the destruction of melanocytes. J Invest Dermatol. 2014 Jan;134(1):183-91.

129.	Zhou R, Tardivel A, Thorens B, Choi I and Tschopp J. Thioredoxin-interacting protein links oxidative stress to inflammasome activation. Nat Immunol. 2010 Feb;11(2):136-40.

130.	Martinon F. Signaling by ROS drives inflammasome activation. Eur J Immunol. 2010 Mar;40(3):616-9.

131.	Simeonova PP and Luster MI. Iron and reactive oxygen species in the asbestos-induced tumor necrosis factor-alpha response from alveolar macrophages. Am J Respir Cell Mol Biol. 1995 Jun;12(6):676-83.

132.   Lo YY, Wong JM and Cruz TF. Reactive oxygen species mediate cytokine activation of c-Jun NH2-terminal kinases. J Biol Chem. 1996 Jun 28;271(26):15703-7.

133.   Yang HH, Chen Y, Gao CY, Cui ZT and Yao JM. Protective Effects of MicroRNA-126 on Human Cardiac Microvascular Endothelial Cells Against Hypoxia/Reoxygenation-Induced Injury and Inflammatory Response by Activating PI3K/Akt/eNOS Signaling Pathway. Cell Physiol Biochem. 2017 Jun 5;42(2):506-518.

134.   Amma H, Naruse K, Ishiguro N and Sokabe M. Involvement of reactive oxygen species in cyclic stretch-induced NF-kappaB activation in human fibroblast cells. Br J Pharmacol. 2005 Jun;145(3):364-73.

135.   Blaser H, Dostert C, Mak TW and Brenner D. TNF and ROS Crosstalk in Inflammation. Trends Cell Biol. 2016 Apr;26(4):249-61.

136.   Fuchs Y and Steller H. Live to die another way: modes of programmed cell death and the signals emanating from dying cells. Nat Rev Mol Cell Biol. 2015 Jun;16(6):329-44.

137.   Inoue S, Browne G, Melino G and Cohen GM. Ordering of caspases in cells undergoing apoptosis by the intrinsic pathway. Cell Death Differ. 2009 Jul;16(7):1053-61.

138.   Bratton SB, Walker G, Roberts DL, Cain K and Cohen GM. Caspase-3 cleaves Apaf-1 into an approximately 30 kDa fragment that associates with an inappropriately oligomerized and biologically inactive approximately 1.4 MDa apoptosome complex. Cell Death Differ. 2001 Apr;8(4):425-33.

139.   Tummers B and Green DR. Caspase-8: regulating life and death. mmunol Rev. 2017 May;277(1):76-89.

140.   Zhang B, Hirahashi J, Cullere X and Mayadas TN. Elucidation of molecular events leading to neutrophil apoptosis following phagocytosis: cross-talk between caspase 8, reactive oxygen species, and MAPK/ERK activation. Biol Chem. 2003 Aug 1;278(31):28443-54.

141.   Wu W, Liu P and Li J. Necroptosis: an emerging form of programmed cell death. Crit Rev Oncol Hematol. 2012 Jun;82(3):249-58.

142.   Van Herreweghe F, Festjens N, Declercq W and Vandenabeele P. Tumor necrosis factor-mediated cell death: to break or to burst, that's the question. Cell Mol Life Sci. 2010 May;67(10):1567-79.

143.   Kim JY, Kim YJ, Lee S and Park JH. BNip3 is a mediator of TNF-induced necrotic cell death. Apoptosis. 2011 Feb;16(2):114-26.

144.   Irrinki KM, Mallilankaraman K, Thapa RJ, Chandramoorthy HC, Smith FJ, Jog NR, Gandhirajan RK, Kelsen SG, Houser SR, May MJ, Balachandran S and Madesh M. Requirement of FADD, NEMO, and BAX/BAK for aberrant mitochondrial function in tumor necrosis factor alpha-induced necrosis. Mol Cell Biol. 2011 Sep;31(18):3745-58.

145.   Takemura R, Takaki H, Okada S, Shime H, Akazawa T, Oshiumi H, Matsumoto M, Teshima T and Seya T. PolyI:C-Induced TLR3/RIP3-Dependent Necroptosis Backs Up Immune Effector-Mediated Tumor Elimination In Vivo. Cancer Immunol Res. 2015 Aug;3(8):902-14.

146.   Legarda D, Justus SJ, Ang RL, Rikhi N, Li W, Moran TM, Zhang J, Mizoguchi E, Zelic M, Kelliher MA, Blander JM and Ting AT. CYLD Proteolysis Protects Macrophages from TNF-Mediated Auto-necroptosis Induced by LPS and Licensed by Type I IFN. Cell Rep. 2016 Jun 14;15(11):2449-61.

147.   De Almagro MC and Vucic D. Necroptosis: Pathway diversity and characteristics. Semin Cell Dev Biol. 2015 Mar; 39:56-62.

148.   Cai Z and Liu ZG. Execution of RIPK3-regulated necrosis. Mol Cell Oncol. 2014 Oct 29;1(2): e960759

149.   Murphy JM, Czabotar PE, Hildebrand JM, Lucet IS, Zhang JG, Alvarez-Diaz S, Lewis R, Lalaoui N, Metcalf D, Webb AI, Young SN, Varghese LN, Tannahill GM, Hatchell EC, Majewski IJ, Okamoto T, Dobson RC, Hilton DJ, Babon JJ, Nicola NA, Strasser A, Silke J and Alexander WS. The pseudokinase MLKL mediates necroptosis via a molecular switch mechanism. Immunity. 2013 Sep 19;39(3):443-53.

150.   Hildebrand JM, Tanzer MC, Lucet IS, Young SN, Spall SK, Sharma P, Pierotti C, Garnier JM, Dobson RC, Webb AI, Tripaydonis A, Babon JJ, Mulcair MD, Scanlon MJ, Alexander WS, Wilks AF, Czabotar PE, Lessene G, Murphy JM and Silke J. Activation of the pseudokinase MLKL unleashes the four-helix bundle domain to induce membrane localization and necroptotic cell death. Proc Natl Acad Sci U S A. 2014 Oct 21;111(42):15072-7.

151.   Bergsbaken T, Fink SL and Cookson BT. Pyroptosis: host cell death and inflammation. Nat Rev Microbiol. 2009 Feb;7(2):99-109.

152.   Dikic I. Proteasomal and Autophagy Degradation Systems. Annu Rev Biochem. 2017 May 1.

153.   Klionsky D and Emr SD. Autophagy as a regulated pathway of cellular degradation. Science. 2000 Dec 1;290(5497):1717-21.

154.   Kim J and Klionsky DJ. Autophagy, cytoplasm-to-vacuole targeting pathway, and pexophagy in yeast and mammalian cells. Annu Rev Biochem. 2000; 69:303-42.

155.   Takahashi Y, Coppola D, Matsushita N, Cualing HD, Sun M, Sato Y, Liang C, Jung JU, Cheng JQ, Mulé JJ, Pledger WJ and Wang HG. Bif-1 interacts with Beclin 1 through UVRAG and regulates autophagy and tumorigenesis. Nat Cell Biol. 2007 Oct;9(10):1142-51.

156.   Kabeya Y, Mizushima N, Ueno T, Yamamoto A, Kirisako T, Noda T, Kominami E, Ohsumi Y, and Yoshimori T. LC3, a mammalian homologue of yeast Apg8p, is localized in autophagosome membranes after processing. EMBO J. 2000 Nov 1;19(21):5720-8.

157.   Seo Y, Cho YS, Huh YD and Park H. Copper Ion from Cu2O Crystal Induces AMPK-Mediated Autophagy via Superoxide in Endothelial Cells. Mol Cells. 2016 Mar;39(3):195-203.

158.   Chen Y, Azad MB and Gibson SB. Superoxide is the major reactive oxygen species regulating autophagy. Cell Death Differ. 2009 Jul;16(7):1040-52.

159.   Scherz-Shouval R and Elazar Z. ROS, mitochondria and the regulation of autophagy. Trends Cell Biol. 2007 Sep;17(9):422-7.

160.   Boya P, González-Polo RA, Casares N, Perfettini JL, Dessen P, Larochette N, Métivier D, Meley D, Souquere S, Yoshimori T, Pierron G, Codogno P and Kroemer G. Inhibition of macroautophagy triggers apoptosis. Mol Cell Biol. 2005 Feb;25(3):1025-40.

161.   Rouschop KM, Ramaekers CH, Schaaf MB, Keulers TG, Savelkouls KG, Lambin P, Koritzinsky M and Wouters BG. Autophagy is required during cycling hypoxia to lower production of reactive oxygen species. Radiother Oncol. 2009 Sep;92(3):411-6.

162.   Ratledge C and Dover LG. Iron metabolism in pathogenic bacteria. Annual Rev Microbiol. 2000; 54:881-941.

163.   Skaar EP. The battle for iron between bacterial pathogens and their vertebrate hosts. PLoS Pathog. 2010 Aug 12;6(8): e1000949.

164.	Palmer LD and Skaar EP. Transition Metals and Virulence in Bacteria. Annu Rev Genet. 2016 Nov 23; 50:67-91.

165.	Gerhard GS, Levin KA, Price Goldstein J, Wojnar MM, Chorney MJ and Belchis DA. Vibrio vulnificus septicemia in a patient with the hemochromatosis HFE C282Y mutation. Arch Pathol Lab Med. 2001 Aug;125(8):1107-9.

166.	Quenee LE, Hermanas TM, Ciletti N, Louvel H, Miller NC, Elli D, Blaylock B, Mitchell A, Schroeder J, Krausz T, Kanabrocki J and Schneewind O. Hereditary hemochromatosis restores the virulence of plague vaccine strains. J Infect Dis. 2012 Oct 1;206(7):1050-8.

167.	Frank KM, Schneewind O and Shieh WJ. Investigation of a researcher's death due to septicemic plague. N Engl J Med. 2011 Jun 30;364(26):2563-4.

168.	Verga Falzacappa MV, Vujic Spasic M, Kessler R, Stolte J, Hentze MW and Muckenthaler MU. STAT3 mediates hepatic hepcidin expression and its inflammatory stimulation. Blood. 2007 Jan 1;109(1):353-8.

169.	Raj DS. Role of interleukin-6 in the anemia of chronic disease. Semin Arthritis Rheum. 2009 Apr;38(5):382-8.

170.	Villarroel P, Le Blanc S and Arredondo M. Interleukin-6 and lipopolysaccharide modulate hepcidin mRNA expression by HepG2 cells. Biol Trace Elem Res. 2012 Dec;150(1-3):496-501.

171.	Nemeth E, Rivera S, Gabayan V, Keller C, Taudorf S, Pedersen BK and Ganz T. IL-6 mediates hypoferremia of inflammation by inducing the synthesis of the iron regulatory hormone hepcidin. J Clin Invest. 2004 May;113(9):1271-6.

172.	Wrighting DM and Andrews NC. Interleukin-6 induces Hepcidin expression through STAT3. Blood. 2006 Nov 1;108(9):3204-9.

173.	Gardenghi S, Renaud TM, Meloni A, Casu C, Crielaard BJ, Bystrom LM, Greenberg-Kushnir N, Sasu BJ, Cooke KS and Rivella S. Distinct roles for hepcidin and interleukin-6 in the recovery from anemia in mice injected with heat-killed Brucella abortus. Blood. 2014 Feb 20;123(8):1137-45.

174.	Goodnough LT, Nemeth E and Ganz T. Detection, evaluation, and management of iron-restricted erythropoiesis. Blood. 2010 Dec 2;116(23):4754-61.

175.   Theurl M, Nairz M, Schroll A, Sonnweber T, Asshoff M, Haschka D, Seifert M, Willenbacher W, Wilflingseder D, Posch W, Murphy AT, Witcher DR, Theurl I and Weiss G. Hepcidin as a predictive factor and therapeutic target in erythropoiesis-stimulating agent treatment for anemia of chronic disease in rats. Haematologica. 2014 Sep;99(9):1516-24.

176.   Lee P, Peng H, Gelbart T, Wang L and Beutler E. Regulation of hepcidin transcription by interleukin-1 and interleukin-6. Proc Natl Acad Sci U S A. 2005 Feb 8;102(6):1906-10.

177.   Zhang X and Rovin BH. Hepcidin expression by human monocytes in response to adhesion and pro-inflammatory cytokines. Biochim Biophys Acta. 2010 Dec;1800(12):1262-7.

178.   Kanamori Y, Murakami M, Sugiyama M, Hashimoto O, Matsui T and Funaba M. IL-1β transcriptionally activates hepcidin by inducing C/EBPδ expression in hepatocytes. J Biol Chem. 2017 Apr 24. pii: jbc.M116.770974.

179.   Oliveira SJ, Pinto JP, Picarote G, Costa VM, Carvalho F, Rangel M, de Sousa M and de Almeida SF. ER stress-inducible factor CHOP affects the expression of hepcidin by modulating C/EBPalpha activity. PLoS One. 2009 Aug 12;4(8): e6618.

180.   Vecchi C, Montosi G, Zhang K, Lamberti I, Duncan SA, Kaufman RJ and Pietrangelo A. ER stress controls iron metabolism through induction of hepcidin. Science. 2009 Aug 14;325(5942):877-80.

181.   Canali S, Vecchi C, Garuti C, Montosi G, Babitt JL and Pietrangelo A. The SMAD Pathway Is Required for Hepcidin Response During Endoplasmic Reticulum Stress. Endocrinology. 2016 Oct;157(10):3935-3945.

182.   Hou CH, Fong YC and Tang CH. HMGB-1 induces IL-6 production in human synovial fibroblasts through c-Src, Akt and NF-κB pathways. J Cell Physiol. 2011 Aug;226(8):2006-15.

183.   Kwak MS, Lim M, Lee YJ, Lee HS, Kim YH, Youn JH, Choi JE and Shin JS. HMGB1 Binds to Lipoteichoic Acid and Enhances TNF-α and IL-6 Production through HMGB1-Mediated Transfer of Lipoteichoic Acid to CD14 and TLR2. J Innate Immun. 2015;7(4):405-16.

184.   Flo TH, Smith KD, Sato S, Rodriguez DJ, Holmes MA, Strong RK, Akira S and Aderem A. Lipocalin 2 mediates an innate immune response to bacterial infection by sequestrating iron. Nature. 2004 Dec 16;432(7019):917-21.

185.   Yang J, Goetz D, Li JY, Wang W, Mori K, Setlik D, Du T, Erdjument-Bromage H, Tempst P, Strong R and Barasch J. An iron delivery pathway mediated by a lipocalin. Mol Cell. 2002 Nov;10(5):1045-56.

186.   Granick S and Michaelis L. Ferritin and Apoferritin. Science. 1942 Apr 24;95(2469):439-40.

187.   Konijn AM and Hershko C. Ferritin synthesis in inflammation. I. Pathogenesis of impaired iron release. Br J Haematol. 1977 Sep;37(1):7-16.

188.   Konijn AM, Carmel N, Levy R and Hershko C. Ferritin synthesis in inflammation. II. Mechanism of increased ferritin synthesis. Br J Haematol. 1981 Nov;49(3):361-70.

189.   Blake DR, Waterworth RF and Bacon PA. Assessment of iron stores in inflammation by assay of serum ferritin concentrations. Br Med J (Clin Res Ed). 1981 Oct 31;283(6300):1147-8.

190.   Gutteberg TJ, Røkke O, Andersen O and Jørgensen T. Early fall of circulating iron and rapid rise of lactoferrin in septicemia and endotoxemia: an early defence mechanism. Scand J Infect Dis. 1989;21(6):709-15.

191.   Blackwell JM. Structure and function of the natural-resistance-associated macrophage protein (Nramp1), a candidate protein for infectious and autoimmune disease susceptibility. Mol Med Today. 1996 May;2(5):205-11.

192.   Borrego A, Peters LC, Jensen JR, Ribeiro OG, Koury Cabrera WH, Starobinas N, Seman M, Ibañez OM and De Franco M. Genetic determinants of acute inflammation regulate Salmonella infection and modulate Slc11a1 gene (formerly Nramp1) effects in selected mouse lines. Microbes Infect. 2006 Oct;8(12-13):2766-71.

193.   Rius J, Guma M, Schachtrup C, Akassoglou K, Zinkernagel AS, Nizet V, Johnson RS, Haddad GG and Karin M. NF-kappaB links innate immunity to the hypoxic response through transcriptional regulation of HIF-1alpha. Nature. 2008 Jun 5;453(7196):807-11.

194.   Tacchini L, Gammella E, De Ponti C, Recalcati S and Cairo G. Role of HIF-1 and NF-kappaB transcription factors in the modulation of transferrin receptor by inflammatory and anti-inflammatory signals. J Biol Chem. 2008 Jul 25;283(30):20674-86.

195.   Raja KB, Duane P and Peters TJ. Effects of turpentine-induced inflammation on the hypoxic stimulation of intestinal Fe3+ absorption in mice. Int J Exp Pathol. 1990 Dec;71(6):785-9.

196.   Langdon JM, Yates SC, Femnou LK, McCranor BJ, Cheadle C, Xue QL, Vaulont S, Civin CI, Walston JD and Roy CN. Hepcidin-dependent and hepcidin-independent regulation of erythropoiesis in a mouse model of anemia of chronic inflammation. Am J Hematol. 2014 May;89(5):470-9.

197.   Connolly KM, Stecher VJ and Kent L. Examination of interleukin-1 activity, the acute phase response, and leukocyte subpopulations in rats with adjuvant-induced arthritis. J Lab Clin Med. 1988 Mar;111(3):341-7.

198.   Shanmugam NK, Ellenbogen S, Trebicka E, Wang L, Mukhopadhyay S, Lacy-Hulbert A, Gallini CA, Garrett WS and Cherayil BJ. Tumor necrosis factor α inhibits expression of the iron regulating hormone hepcidin in murine models of innate colitis. PLoS One. 2012;7(5): e38136.

199.   Wizorek JJ, Turnbull IR and Buchman TG. Iron overload before cecal ligation and puncture increases mortality. Shock. 2003 Jul;20(1):52-5.

200.   Rivera S and Ganz T. Animal models of anemia of inflammation. Semin Hematol. 2009 Oct;46(4):351-7

201.   Frazer DM, Wilkins SJ, Millard KN, McKie AT, Vulpe CD, Anderson GJ. Increased hepcidin expression and hypoferraemia associated with an acute phase response are not affected by inactivation of HFE. Br J Haematol. 2004;1 26:434–436.

202.   Mikolajew M, Stachurska J, Kalczak M, Lewicka S, Kossakowska M. Hematologic changes in rats with adjuvant-induced disease. Intravascular clotting and fibrinolysis as a possible factor in the pathogenesis of anemia. Reumatologia. 1975; 13:47–56.

203.   Montosi G, Corradini E, Garuti C, Barelli S, Recalcati S, Cairo G, et al. Kupffer cells and macrophages are not required for hepatic hepcidin activation during iron overload. Hepatology. 2005; 41:545–552.

204.   Sasu BJ, Cooke KS, Arvedson TL, Plewa C, Ellison AR, Sheng J, Winters A, Juan T, Li H, Begley CG and Molineux G. Antihepcidin antibody treatment modulates iron metabolism and is effective in a mouse model of inflammation-induced anemia. Blood. 2010 Apr 29;115(17):3616-24.

205.   Kim A, Fung E, Parikh SG, Valore EV, Gabayan V, Nemeth E and Ganz T. A mouse model of anemia of inflammation: complex pathogenesis with partial dependence on hepcidin. Blood. 2014 Feb 20;123(8):1129-36.

206.   Fraenkel PG. Critical models for the anemia of inflammation. Blood. 2014 Feb 20;123(8):1124-5

207.   Kautz L, Jung G, Nemeth E and Ganz T. Erythroferrone contributes to recovery from anemia of inflammation. Blood. 2014 Oct 16;124(16):2569-74.

208.   Kim A, Fung E, Parikh SG, Gabayan V, Nemeth E, and Ganz T. Isocitrate treatment of acute anemia of inflammation in a mouse model. Blood Cells Mol Dis. 2016 Jan;56(1):31-6.

209.   Pan H, Xu X, Hao X and Chen Y. Changes in myogenic reactive oxygen species and interleukin-6 in contracting skeletal muscle cells.

210.   Kosmidou I, Vassilakopoulos T, Xagorari A, Zakynthinos S, Papapetropoulos A and Roussos C. Production of interleukin-6 by skeletal myotubes: role of reactive oxygen species. Am J Respir Cell Mol Biol. 2002 May;26(5):587-93.

211.   Henríquez-Olguín C, Altamirano F, Valladares D, López JR, Allen PD and Jaimovich E. Altered ROS production, NF-κB activation and interleukin-6 gene expression induced by electrical stimulation in dystrophic mdx skeletal muscle cells. Biochim Biophys Acta. 2015 Jul;1852(7):1410-9.

212.   Altamirano F, López JR, Henríquez C, Molinski T, Allen PD and Jaimovich E. Increased resting intracellular calcium modulates NF-κB-dependent inducible nitric-oxide synthase gene expression in dystrophic mdx skeletal myotubes. J Biol Chem. 2012 Jun 15;287(25):20876-87.